

Advanced model for simulating the dynamic behavior of the mesh

Master Thesis in automotive engineering



Author: Alberto Pesando (Student ID: s250031)

Supervisor: Prof. Carlo Rosso

Co-Supervisor: Ing. Claudio Marcellini, Ing. Fabio
Bruzzone, Ing. Tommaso Maggi

Politecnico di Torino

October 08, 2019

Acknowledgements

I would first like to thank my thesis supervisor Prof. Carlo Rosso for his fundamental help, Prof. Rosso has been always open to listen to my doubts and help me when I've been through some difficulties. He made me able to create my own work, but he pointed out to me the right direction whenever I needed it.

I would also like to thank my co-supervisors Ing. Claudio Marcellini, Ing. Fabio Bruzzone and Ing. Tommaso Maggi who shared with me their knowledge and ideas, devoting their time and effort to help me finishing my work in the best way possible.

I want also to express my profound gratitude and unconditional love for my family: my parents Gianna and Gabriele, my grandmothers Elia and Lidia, my grandfather Antonio, my uncle Paolo, my aunt Chanel and my girlfriend Lucia. They greatly supported me not only in the development of this work but in all these years of study and through my all life with love and efforts, making me able to follow my many passions and fulfill my goals, always motivating and trusting me. None of what I've done could have been possible without you.

To who I consider my other family, my friends, who accompanied me in my growth path and through the years I can't say anything but a huge thank you, you are a part of me and of who I am. Thank you for being with me and never letting me down.

Finally a thank you from the bottom of my heart and a big hug to my grandfather Carlo, you couldn't be physically present throughout this last year but this didn't matter on the impact you had on my life and my way of being. I love you.

Summary

The environment regarding the work I have done is the study of the dynamic behaviour of two meshing gears and the way their parameters affect the functioning of the gear couple.

Many parameters needed to be analyzed, first of all I needed to be able to calculate the dynamic force acting between the two gears, their displacements and the stresses they have to bear all in a single model that could work independently from the input given and able to be fed with whatever data the user wants.

The flexibility of the system regarding input data was a must in order to make the system as flexible as possible, but also in order to be able to observe as many phenomena as possible having a huge variety of functions all implemented in a single signal path.

The task has been accomplished using Simulink, a MatLab extension for graphical interface software that can be fed with MatLab code in order to execute calculations remaining easy to understand by eye and also being quite fast to run in comparison to many other softwares available.

The main purpose of this work is to build a reliable Simulink model able to simulate the dynamic behaviour of two meshing gears accordingly with experimental data and theoretical concepts but also operating a fast and easy way for the hardware to compute. The target of this model is to give an overview of the main phenomena acting between the meshing gears and evaluate its effects on endured stresses, wear, functioning and noise

Contents

Acknowledgements	I
Summary	III
List of figures	IX
1 Introduction	1
1.1 Introduction to simulink	1
1.1.1 Most used Simulink blocks	3
1.2 Introduction to gears	7
1.2.1 Gear tooth and its geometry	8
1.3 Analysis of the nonlinear behavior of gear pairs	10
1.4 Dynamic analysis of gears	15
2 Simulink Model	20
2.1 General overview of the model	20
2.2 Analysis and purpose of the various subsystems	22
2.2.1 Subsystem 1 and STE calculation	22
2.2.2 Subsystem 2	26
2.2.3 Switch	28
2.2.4 Final operations and output	32
3 Torque inversion	33
3.1 Implementation of the model	33
3.1.1 Input torque determination	34
3.1.2 Torque switch selector	37
3.1.3 Dynamic force calculation - positive torque	38
3.1.4 Dynamic force calculation - negative torque	40
3.1.5 Final section and overall dynamic force	40

4 Simulations	42
4.1 Simulations without torque inversion	42
4.1.1 Simulations settings	42
4.1.2 Simulink settings	43
4.1.3 Simulations results	45
4.2 Simulations with torque inversion	50
4.2.1 Simulations settings	50
4.2.2 Simulations results and vibration analysis . . .	52
4.2.2.1 Speed at 600 rpm	52
4.2.2.2 Speed at 1200 rpm	55
4.2.2.3 Speed at 1800 rpm	58
4.2.2.4 Speed at 3800 rpm	61
4.2.2.5 Speed at 6000 rpm	64
4.3 Further simulations	68
4.3.1 Step inputs	68
4.3.2 Double ramp input	72
Conclusions	77
Appendix: Matlab configuration workspace	79
References	81

List of Figures

1	Simulink block library window	2
2	Constant source block	3
3	Ramp source block	3
4	Step source block	4
5	Scope block	4
6	Integrator block	4
7	Absolute value block	5
8	Square root block	5
9	Integrator block	5
10	Floor function block	5
11	Switch block	5
12	2-D Lookup Table block	6
13	Gear nomenclature	7
14	Gear's tooth nomenclature	9
15	Torque-force relations	11
16	Schematic diagram of a gear pair	12
17	Schematic lubricant film parameters	12
18	Schematic contact area parameters	13
19	Mesh stiffness and LOA: (a) rectangular type mesh stiffness (b) distance from starting point A along the LOA (c) distance as function of time per tooth mesh cycle	14
20	Tuplin's model	16
21	Houser and <i>Özgülven's model</i>	18
22	Non linear elastic force of teeth	19
23	Simulink model	20
24	Ramp settings window	21
25	Example of output of a scope block	21
26	Subsystem division of complete model	22
27	Subsystem 1	22

28	2-D Lookup Table	23
29	Look-up table parameters panel 1	24
30	Look-up table parameters panel 2	24
31	Look-up table parameters panel 3	25
32	Subsystem 2	26
33	Non linear elastic force of teeth	27
34	Stiffness evaluating subsystem	28
35	Switch subsystem	29
36	Comparation to constant block	29
37	Comparation to constant user panel	29
38	Interval test block	30
39	Interval test block panel	30
40	Switch block	31
41	Switch block panel	31
42	Final output of the model	32
43	Torque inversion model	34
44	Constant torque input blocks	34
45	Inversion ramp block panel	35
46	Torque input result	36
47	Varying torque input blocks	36
48	Torque input result with ramp blocks	37
49	Torque switch selector	38
50	Positive dynamic force contribution subsystem	39
51	Detail of the positive dynamic force contribution subsystem	39
52	Negative dynamic force contribution subsystem	40
53	Final operations to get the overall dynamic force value	41
54	Simulink configuration parameters window	44
55	Configuration properties of scope blocks	44

56	Data entering the 2-D lookup table representing the instantaneous position between gear teeth	45
57	Static transmission error STE	46
58	Displacements	46
59	Calculated gear stiffness	47
60	Damped force contribution	47
61	Non damped force contribution	48
62	Overall dynamic force between meshing gears	48
63	Dynamic force in function of time	51
64	Instantaneous position between two gear teeth coming out of Subsystem 1	53
65	STE values before and after torque inversion at 600rpm	53
66	Contribution of damping at 600 rpm, before and after torque inversion	54
67	Dynamic force at 600 rpm	55
68	Instantaneous position between two gear teeth coming out of Subsystem 1	56
69	STE values before and after torque inversion at 1200rpm	56
70	Contribution of damping at 1200 rpm, before and after torque inversion	57
71	Dynamic force at 1200 rpm	57
72	Instantaneous position between two gear teeth coming out of Subsystem 1	58
73	STE values before and after torque inversion at 1800rpm	58
74	Contribution of damping at 1800 rpm, before and after torque inversion	59
75	Dynamic force at 1800 rpm	59
76	Detail of vibration caused by dynamic force at 1800 rpm	60
77	Dynamic force at 1800 rpm without vibration using damping factor 0.14	60
78	Instantaneous position between two gear teeth coming out of Subsystem 1	61

79	STE values before and after torque inversion at 3800rpm	62
80	Contribution of damping at 3800 rpm, before and after torque inversion	62
81	Dynamic force at 3800 rpm	63
82	Detail of vibration caused by the dynamic force at 3800 rpm	63
83	Dynamic force at 3800 rpm without vibration using damping factor=0.2	64
84	Instantaneous position between two gear teeth coming out of Subsystem 1	65
85	STE values before and after torque inversion at 6000rpm	65
86	Contribution of damping at 6000 rpm, before and after torque inversion	66
87	Dynamic force at 6000 rpm	67
88	Step input for torque values, T fixed to 100Nm	68
89	Step input for speed values, every single constant block expresses rotational speed in rad/s	69
90	Torque input values	70
91	Speed input values	70
92	Instantaneous position of the teeth	71
93	STE values	71
94	Overall dynamic force	72
95	Torque input blocks	73
96	Speed input blocks	73
97	Torque input value	74
98	Speed input value	74
99	Instantaneous position of the teeth	75
100	STE before and after torque inversion	76
101	Overall dynamic force	76

1 Introduction

This first introduction deals with a generic description of what was necessary for understanding the starting point of the project and begin working on this thesis and on the model.

First of all here is an introduction on the program used for "building" the model, Simulink, a very useful and quite user-friendly MatLab extension able to represent functional blocks in a very clear way, specifying their function and the signal path in a way that is easier for the user to understand and to modify when needed.

Second part of the introduction will face the trickiest part of the work, it will in fact introduce the gear meshing theory and its evolution in many years of research, in order to be able to understand assumptions and thoughts all along the explanation of my work.

1.1 Introduction to simulink

Simulink (Simulation and link) is developed by MathWorks as an add-on with MATLAB.

It is a graphical programming language which offers modelling, simulation and analyzing of multi domain dynamic systems under Graphical User Interface (GUI) environment. The Simulink have tight integration with the MATLAB environment and have a comprehensive block libraries and toolboxes for linear and nonlinear analyses; system models can be so easily constructed via just click and drag operations. The Simulink comes handy while dealing with control theory and model based design.

In Simulink, it is very straightforward to represent and then simulate a mathematical model representing a physical system. Models are represented graphically in Simulink as block diagrams.

A wide array of blocks are available to the user in provided libraries for representing various phenomena and models in a range of formats. One of the primary advantages of employing Simulink (and simulation in general) for the analysis of dynamic systems is that it allows us to quickly analyze the response of complicated systems that may be prohibitively difficult to analyze analytically.

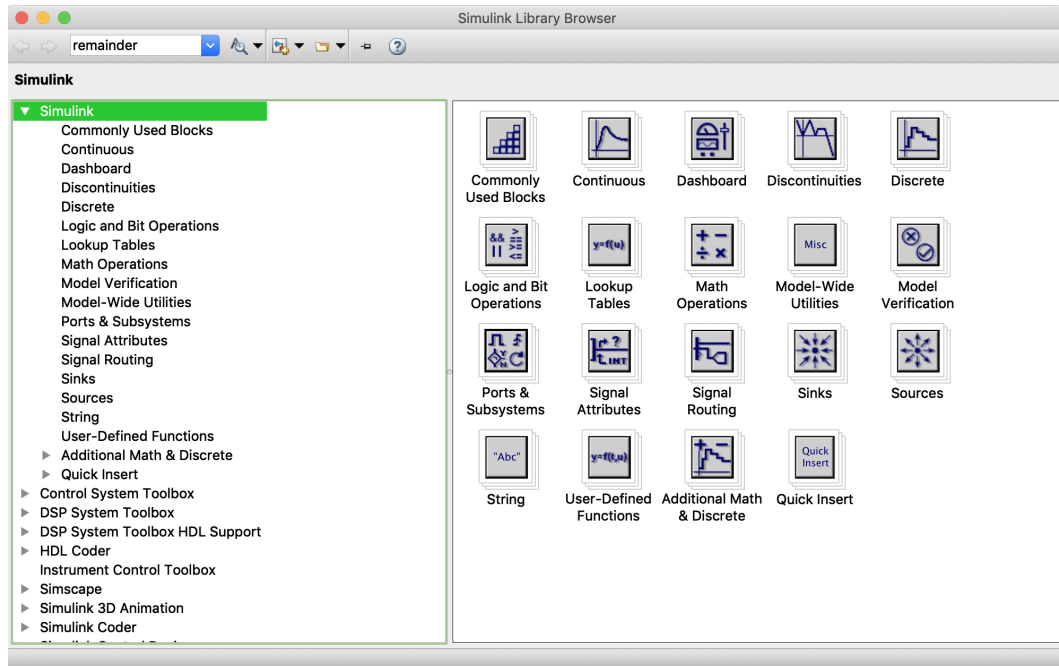


Figure 1: Simulink block library window

In all Simulink library there are many many functions that can be accomplished by Simulink blocks, starting from simple mathematical operations such as additions or multiplications to very complex lookup tables, every function is encapsulated in simple blocks that are very easy to place and order, in order to make a signal path clear to understand and to modify when needed.

Also, Simulink allows you to incorporate MATLAB algorithms into models as well as export the simulation results into MATLAB for further analysis as has been done for this work, for example it supports:

- system-level design
- simulation
- automatic code generation
- testing and verification of embedded systems

All this functions are included in a very user-friendly interface of work, that makes the user able to place and link every block easily simply with a drag and drop of the interested blocks from the library page into the work field. Every block can be associated with variables or calculations coming from Matlab code.

1.1.1 Most used Simulink blocks

In this section the most common Simulink blocks used in this work are shown, many others are present in Simulink library but I wanted to keep the model as slim as possible in order to run faster and to be the least complex as possible in architecture.

The main block's types I used to model and run this system simulation are:

- Source blocks
- Output or sink blocks
- Math operations blocks
- Signal attributes blocks
- Signal routing blocks

First of all we have source blocks which are meant to give us an input for the whole system; they can represent a constant source (Figure2), a ramp source (Figure3) which outputs a ramp signal, starting at the specified time, a step source (Figure4) or many others.

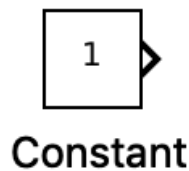


Figure 2: Constant source block



Figure 3: Ramp source block

Moving on, the most used output block used in this model is the scope (Figure5), that can display the quantity we are measuring in time domain and give us a graphic representation of it.

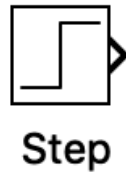


Figure 4: Step source block



Figure 5: Scope block

Other very common blocks are mathematical operations; in the following lines are represented the integrator, the gain, the square root, the absolute value and the rounding function.

Integrator (Figure6), absolute value (Figure7) and square root (Figure8) are pretty straight forward considering the names; for what regards the gain block (Figure9) it gives a element-wise gain output ($y = K \cdot u$) or matrix gain and, at last, the rounding function (Figure10) (in this case floor function has been used) rounds each input element to the nearest integer less than or equal to that element.

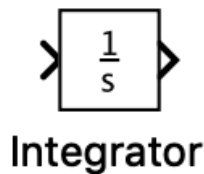


Figure 6: Integrator block

Then we have blocks used to influence the signal path, in this particular case is reported a switch block (Figure11) which can make the signal pass through input 1 when input 2 satisfies the selected criterion; otherwise, it will pass through input 3. The inputs are numbered top to bottom (or left to right). The first and third input ports are data ports, and the second input represents the control port. The criteria for control port 2 are $u_2 \geq \text{threshold}$, $u_2 > \text{threshold}$ or $u_2 = 0$

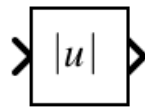
**Abs**

Figure 7: Absolute value block

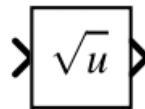
**Sqrt**

Figure 8: Square root block

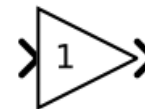
**Gain**

Figure 9: Integrator block

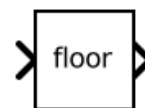
**Rounding
Function**

Figure 10: Floor function block

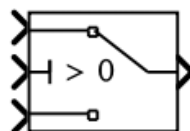
**Switch**

Figure 11: Switch block

The last and more complex element of the Simulink library I used is a 2-D lookup table block (Figure 12) that has the function of performing a n-dimensional interpolated table lookup including index searches. The table is a sampled representation of a function in N variables. Break-point sets relate the input values to positions in the table where the first dimension corresponds to the top (or left) input port.

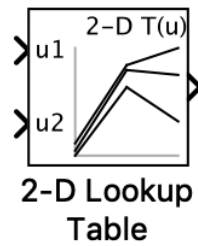


Figure 12: 2-D Lookup Table block

1.2 Introduction to gears

The geared wheel or the gear is usually composed by a series of teeth, a rim, a web and an hub.

The teeth are elements that allowed the motion propagation between the coupled gears; they have a shape that can be assimilated to a beam, and, as a beam, it is subjected to flexural, shear and normal loads.

Gears are usually represented on the basis of they module “m” and the well known relationship between module and number of teeth “z” provides another important parameter of gear: the pitch diameter; from module also depends the height of the tooth, usually considered standard, but that can be modified in order to improve kinematic and resistance properties of the gears.

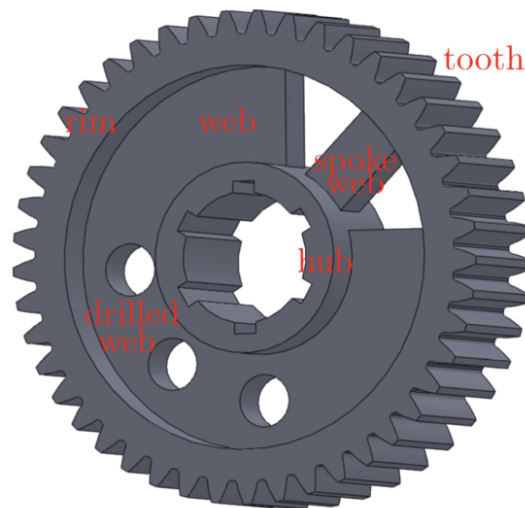


Figure 13: Gear nomenclature

The rim is a ring shape element with usually a rectangular cross section and it is the support of teeth and it represents the element that connects teeth to the rest of the gear.

The web is the part that transmits torque from rim to hub, it is a particular component because it principally endures torque, so it could be very thin with respect to the rest of the gear; it could be drilled or made with a series of beam that connect the rim to the hub.

The hub is the mechanical system that connects geared wheel to shaft, it is usually made by a cylinder with an interface with the shaft that could have a spline coupling, a shrink connection or a key connection.

1.2.1 Gear tooth and its geometry

In this section, an overview of the main tooth parameters is presented. The symbols are in conformity with the ISO standards and are represented in figure 14.

The main important parameter of gears is the pitch diameter “ d ”, it is the quantity that defines the kinematic behavior of gear and the gear ratio. Strictly related to the pitch diameter is the base diameter $d_b = d \cos(\psi)$, where ψ is the pressure angle, that represents the direction along the forces between mating teeth are exchanged. The height “ h ” and the thickness “ s ” of tooth are usually related each other and dependent on the module.

The height of the tooth is divided in two elements, the addendum h_a , that is the upper part of the tooth, from the pitch diameter to the tip, and the dedendum h_f , the part of the tooth from the pitch diameter to the root. Usually, those parameters are strictly related to the module, but some optimization processes can vary that standardized ratios in order to improve the kinematic efficiency and to reduce the wear and noise.

The tooth thickness is usually set as a proportion of the module, result could be changed using profile correction in order to improve load carrying capability of tooth or to avoid cutting interference for gears with little number of teeth.

Very important parameters in the gear dynamic, as highlighted in the following, are the clearances needed for the correct operation of the engagement. One of them is the backlash, in figure 14 the normal backlash j_n is depicted, it represents the gap between two mating surfaces; it is relevant because it is not possible to have negative (that means having interference between the mating surfaces) or zero backlash (that represents the precise contact between the two mating teeth), in fact backlash has to be created for allowing the engagement in presence of natural geometric and manufacturing tolerances. The higher is the gear manufacturing quality, the lower is the backlash, because the lower are the tolerances used in the gear production process, the lower could be the backlash.

The second clearance parameter is the distance between the tooth tip and the root fillet of the mating space between teeth “ c ”, this last

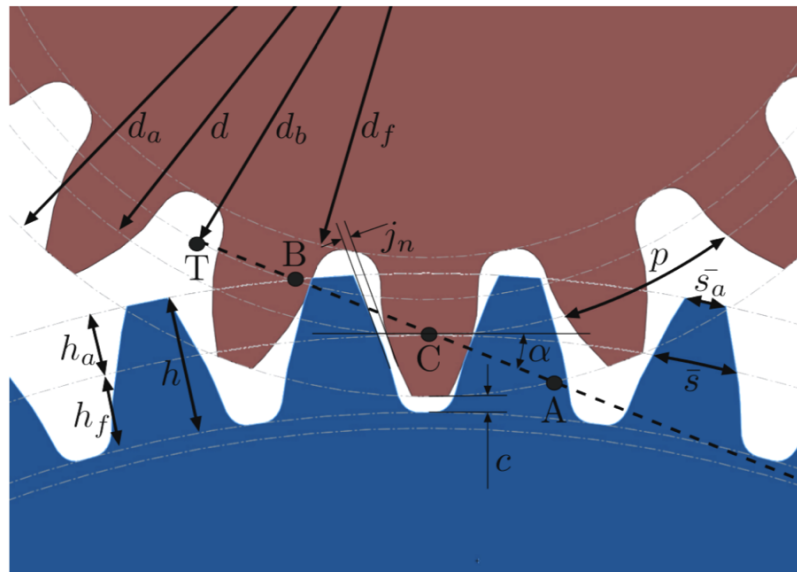


Figure 14: Gear's tooth nomenclature

clearance is important for avoiding interference and for facilitating the lubrication.

Other important parameter for the gear dynamic is the contact ratio, that highlights the number of teeth pair in contact during the engagement. The distance between the point A and B of figure 14 is the contact length, in other words it is the resulting the line of action interested by the teeth mating.

The contact ratio is defined as the ratio between the length of the contact segment AB and the pitch “p”. It is easily understandable that as the contact ratio increases, in the same way the smoothness of the engagement increases, so the dynamic behavior of the mating elements is improved.

1.3 Analysis of the nonlinear behavior of gear pairs

Many previous studies regarding the dynamic behavior of gear pairs have been based on modeling tooth contact as a spring and damper system, with the stiffness of the equivalent spring based on elastic deformation such as Hertzian deformation or tooth bending; however, there has been little research into the effects of sliding friction or the hydrodynamic forces on the dynamic behavior of gear pairs.

Most of the research on gear dynamics uses tooth stiffness based on tooth deformation by direct solid contact and some studies have modeled the tooth stiffness as a constant through the complete tooth contact period with a nonlinear function, assuming that the contact reaction force between the teeth is zero when they are separated from each other.

However, as almost all gear systems are operated under fluid lubrication, a reaction force between the teeth due to the squeeze film effect will occur even when the two solid surfaces are not in contact. Therefore, it seems reasonable to consider the elasto-hydrodynamic lubrication effect between contacting teeth in analysis of the dynamic behavior of gear pair systems.

For what regards the mathematical model of the system consisted of two gears mounted on well-aligned input and output shafts.

The gears were standard errorless involute spur gears with no modifications, and the gear pair was modeled as a purely torsional vibration system. The gears were assumed to be fully lubricated by Newtonian lubricant, and shear force was ignored.

For simplicity of calculation, the conditions of isothermal incompressibility and constant viscosity were assumed. The torque and speed of the input shaft were assumed to be constant. The equations of motion of the two gears were as follows:

$$T_d - T_{mp} = I_p \ddot{\theta}_p \quad (1)$$

where looking at figure 15

T_d and T_o are the static driving and load torques, while T_{mp} and T_{mg} are torques due to tooth meshing forces by the pinion and gear, respec-

$$\begin{aligned}
T_{mp} &= \begin{cases} F_{en}r_p - T_{efp}, & |r_p\theta_p - r_g\theta_g| \geq b \\ F_{hm}r_p - T_{hfp}, & |r_p\theta_p - r_g\theta_g| < b \end{cases}, \\
T_{mg} &= \begin{cases} F_{en}r_g - T_{efg}, & |r_p\theta_p - r_g\theta_g| \geq b \\ F_{hm}r_g - T_{hfg}, & |r_p\theta_p - r_g\theta_g| < b \end{cases}, \\
F_{en} &= k(t)(r_p\theta_p - r_g\theta_g) + c(r_p\dot{\theta}_p - r_g\dot{\theta}_g)
\end{aligned}$$

Figure 15: Torque-force relations

tively. The pinion and gear have base circle radii r_p and r_g , and mass moments of inertia of I_p and I_g , respectively.

The total backlash is $2b$, and parameters $_p$ and $_g$ represent the vibrations of the gears about the nominal rigid body rotation. The forces F_{en} and F_{hm} are normal forces acting along the line of action (LOA) due to elastic deformation and the hydrodynamic effect, respectively.

T_{efp} and T_{hfp} are the torques acting on the pinion induced by the direct contact friction force F_{ef} and the hydrodynamic friction force F_{hf} , respectively. T_{efg} and T_{hfg} are the torques acting on the gear induced respectively by the direct contact friction force F_{ef} and the hydrodynamic friction force F_{hf} .

The general Reynolds equation was used to calculate the hydrodynamic normal force F_{hm}

$$\frac{\delta}{\delta x} \left(\frac{\rho h^3}{12\mu} \frac{\delta p}{\delta x} \right) + \frac{\delta}{\delta y} \left(\frac{\rho h^3}{12\mu} \frac{\delta p}{\delta y} \right) = \frac{\delta}{\delta x} \left[\frac{\rho h(u_a + u_b)}{2} \right] + \frac{\delta}{\delta y} \left[\frac{\rho h(v_a + v_b)}{2} \right] + \frac{\delta(\rho h)}{\delta t} \quad (2)$$

obtaining:

$$F_{hf} = \frac{\pi b \mu_0 u_s}{2} \sqrt{\frac{R}{h}} \quad (3)$$

where u_s is the sliding velocity of the mating gears.

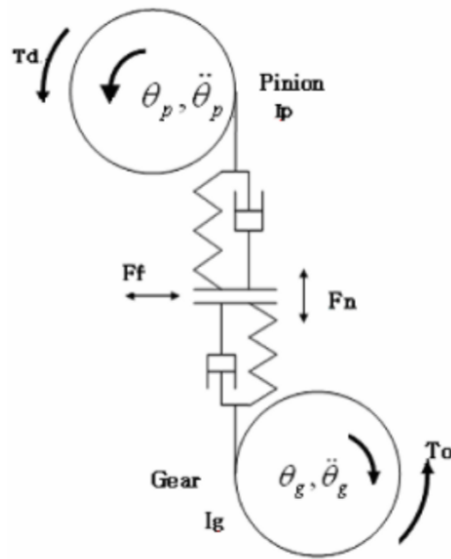


Figure 16: Schematic diagram of a gear pair

Assuming full lubrication, the film thickness is equal to the distance between the two flanks as a function of ξ due to the flank curvature, and is expressed as follows:

$$h = x + \frac{\xi^2}{R} \tag{4}$$

where x is the minimum distance between two flanks at $\xi = 0$.

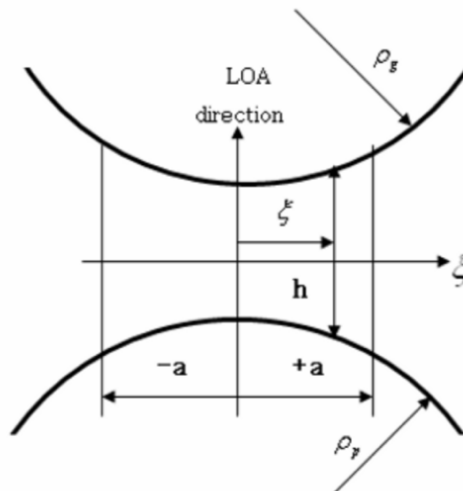


Figure 17: Schematic lubricant film parameters

Parameter x and the DTE are defined as

$$x = b - DTE \tag{5}$$

$$DTE = \theta_p r_p - \theta_g r_g \tag{6}$$

where $2b$ is the total backlash.

The equivalent radius of the contacting point R is defined as

$$R = 2 \frac{\rho_p \rho_g}{\rho_p + \rho_g} \tag{7}$$

where p and g are the pinion surface radii of curvature in the transverse plane, respectively.

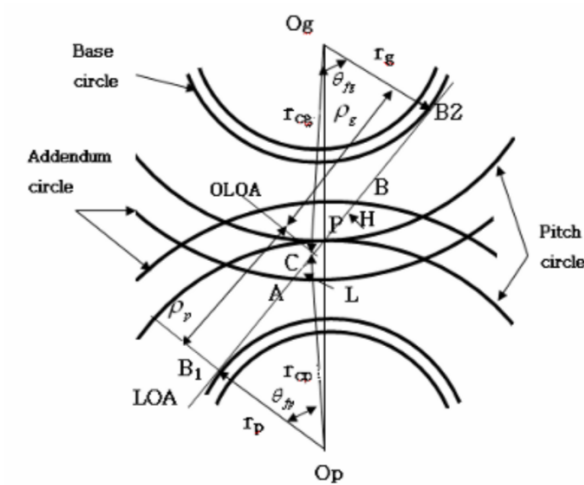


Figure 18: Schematic contact area parameters

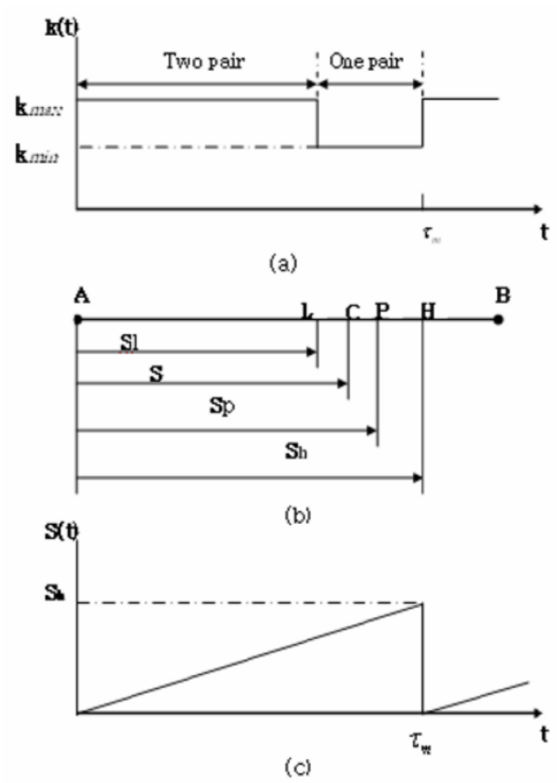


Figure 19: Mesh stiffness and LOA: (a) rectangular type mesh stiffness (b) distance from starting point A along the LOA (c) distance as function of time per tooth mesh cycle

1.4 Dynamic analysis of gears

The first methods to study the gear dynamics were principally experimental and were used to define a factor (the Dynamic Factor or Speed Factor) to scale the nominal force and to take into account the dynamic effect for the design of the gear. The first definition of Dynamic Factor was drawn by comparing the nominal condition to the failure conditions.

In other words, experimental campaigns were set up varying spin speed and load and recording the ruptures. When ruptures occurred, the operating conditions were compared with the nominal ones and the Dynamic Factor was computed.

From the first experiences it clearly appeared that the spin speed is the principal cause of dynamic overload, so an analytical expression of the Dynamic Factor was computed:

$$DF = \frac{78 + \sqrt{v}}{78} = \frac{Load_{dynamic}}{Load_{static}} \quad (8)$$

that is the starting point for the AGMA standard, where the expression of the Dynamic Factor takes into account the manufacturing quality.

The first work that tried to consider the gear manufacturing error was performed by Tuplin.

The model proposed in that work is simple, result well expresses the fundamental of gears mating. In fact, considering an easy two-masses-one-spring model, Tuplin defines the natural frequency of the resonance phenomenon that could occur in a gear pair when a pitch is present and the maximum external load that the gear pair could experience. By referring to the sketch of figure 20, the displacements x_1 and x_2 of the two mating gears can be computed solving a motion equation where the external load is represented by the time variation of the distance between the gear m2 and the stiffness k.

In formula:

$$\left(\frac{d^2}{dt^2} + k\left(\frac{1}{m_2} + \frac{1}{m_1}\right)\right)(x_2 - x_1) = k\left(\frac{1}{m_2} + \frac{1}{m_1}\right)(s + vt) \quad (9)$$

where s is the initial value of the pitch error and v is the time variation of it.

Equation (9) is in the classical form of dynamic function, so the term

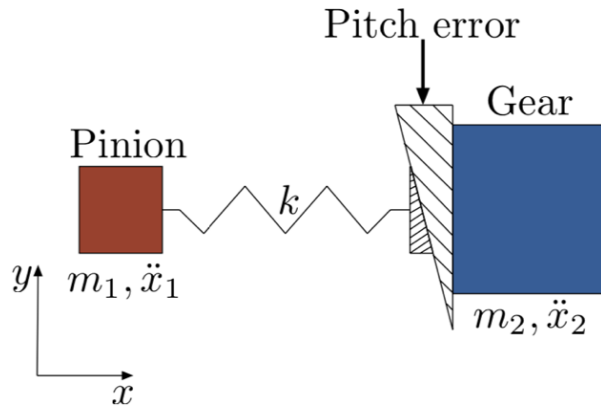


Figure 20: Tuplin's model

$$k\left(\frac{1}{m_2} + \frac{1}{m_1}\right) \quad (10)$$

represents the harmonic characteristic of the function and it becomes the fundamental frequency of the phenomenon:

$$w_n = \sqrt{k \frac{m_1 + m_2}{m_2 m_1}} = \sqrt{k \left(\frac{J_1 r_{b,2}^2 + J_2 r_{b,1}^2}{J_1 J_2} \right)} \quad (11)$$

where J_1 and J_2 are the polar inertias of the two mating gears and $r_{b,i}$ are the base radii of the two gears.

After Tuplin's analysis of the phenomenon others approached the topic in more specific studies; one of the most important papers on the gear dynamics is the work of Harris, where a series of tests were carried out in order to understand the causes of gear vibrations.

Harris analyzed the "relative displacement" as the variation in the velocity ratio at the pitch diameter providing data for different gears and loads. He underlines that the "relative displacement" at a precise load is strictly related to the static error at that load and the differences between the curves he registers at different loads are only related to the variation in stiffness. Important observations he makes are that "the periods during which one or two pairs of teeth are in contact vary with the applied load", and "where the teeth lose contact there is a discontinuity in stiffness". As a consequence of the tests Harris makes some important notes are here reported:

- the dynamic increment of load in gears engagement is inversely dependent on the load amplitude, result never exceed twice the load that gives no error in the velocity ratio;
- if the deflection under load is constant and no errors are present, gears may however oscillate; this is due to the variation of the stiffness during engagements;
- a periodic error under a given load starts vibration when error harmonic is close to the natural frequency of the gears, defining, for a 10% critical damping, an oscillation that could be five times the error;
- The natural frequency of gears depends on the gear mass and the tooth stiffness, this last changes with position of engagement, but the experimental results underline that the natural frequency is more or less the value computed with the mean stiffness.

A little later, in 1978, Wang analyzes the effects of backlash and static transmission error in lightly loaded high speed gears. One of the most important definitions given in those publications is the mechanism a tooth makes during the vibration. The tooth, in presence of backlash and static transmission error, can maintain the adhesion with the mating tooth or can impact and rebound. During impact, two mechanisms take place: momentum transfer and energy consumption.

In absence of transmission error, the impact excitation is vanishing, so the energy that causes the vibration is given by the transmission error.

The final equation that expresses force variation with respect to time considers the Hertzian deformation of teeth, the torsional compliance of gears (in terms of the shaft compliance) and the flexural behavior of the teeth. This expression has to be solved numerically and it provides a trend of tooth load during engagement. This particular expression is able to highlight the variation of loads and the temporary disengagement due to the lose of contact.

That paper was a good starting point for understanding the development of gear studies and it surely is the bases of Houser and Özgüven work. The model presented by Özgüven and Houser is more or less the same proposed before, but it makes the distinction between Static TE and Dynamic TE, the latter computed starting from the first one.

The starting conditions are the same of many other works but stiffness variation and the external loads are expressed in a different way; the problem of varying

pair stiffness is solved considering it as a constant and they also neglect the torque variation, so they can highlight the difference between the STE and DTE. For doing that, authors had to write equilibrium for each wheel around the rotation axis and considering two different excitations e_1 and e_2 .

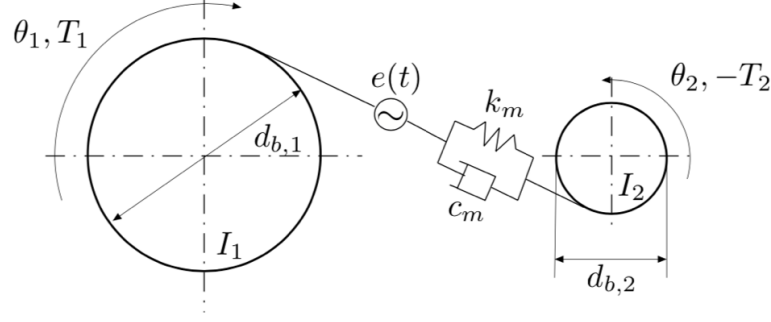


Figure 21: Houser and Özgüven's model

Dividing the contribution in Static and Dynamic Transmission Error, it is possible to write:

Static Transmission Error (STE):

$$x_s = \frac{P_{r,b}}{k_m} + \frac{k_1 e_1 + k_2 e_2}{k_m} \quad (12)$$

Dynamic Transmission Error (DTE):

$$x = x_s + CdP_{r,b}^d + dP_{r,b}^d dC - \frac{c_m \dot{x}}{k_m} - \frac{c_1 \dot{e}_1 + c_2 \dot{e}_2}{k_m} \quad (13)$$

where C represents the meshing compliance and Pd is the dynamic component of exchanged force inside the engagement.

Once computed the displacement and velocity inside the engagement, it is possible to compute the variation of force due to dynamics, as

$$P_{r,b}^d = P_{r,b} + \frac{x - x_s}{C} + 2\zeta \sqrt{\frac{m_e}{C}} \dot{x} \quad (14)$$

The algorithm implemented by Houser and Özgüven considers non linearity in the engagement by using two different mating conditions. In one condition the teeth are in contact and the stiffness is defined and differs from zero, in the other condition, when the teeth are separated, the stiffness and the damping values are equal to zero, so the motion equation in this condition is just defined as

$$m_e \ddot{x} = P_{r,b} \quad (15)$$

The most important result of Houser and Özgüven work is that by neglecting the stiffness variation during engagement, but considering the excitation due to STE the dynamic behavior of gears can be predicted. In other words, the simplification of neglecting the stiffness non linearity due to force application point variation and the idea to use the STE as source bring to a model substantially equivalent to a complex one, where stiffness variation is taken into account.

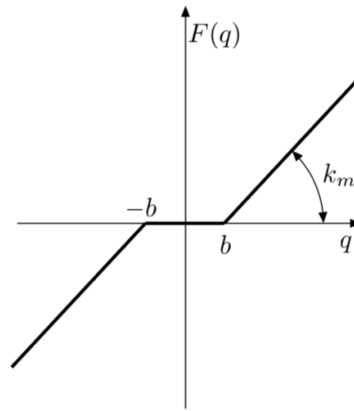


Figure 22: Non linear elastic force of teeth

In addition, Kahraman and Singh demonstrate that the constant viscous damping gives the same results of the more sophisticated damping model, concluding that there is no good reason to use more accurate damping model, helping to simplify the model comprehension.

Another Blankenship and Kahraman work added more specific results to the model a little later; test rig were created in order to test the fundamental equations discussed in the previous works. The numerical results reported in this paper highlight that the higher is the harmonic variation of the stiffness, the higher is the jump effect both on the mean and alternate parts of displacement.

The most important result highlighted here is the influence of the harmonic content of the stiffness on the jump phenomenon. If the stiffness is constant, the preload has a stabilizing effect, so if the jump phenomenon is present in a certain condition, by increasing the preload value, the jump phenomenon tends to disappear.

2 Simulink Model

In this section I will cover the software system generation, explaining the overall architecture of the model, the reason of the usage and placement of various blocks and the composition of subsystems in order to reach the target imposed.

First of all an introduction to the complete model, in order to explain the signal path and calculation that will run in simulations that will be treated later on; then a more in depth analysis of the logic behind the creation of the various subsystems and their main functions all along the model.

2.1 General overview of the model

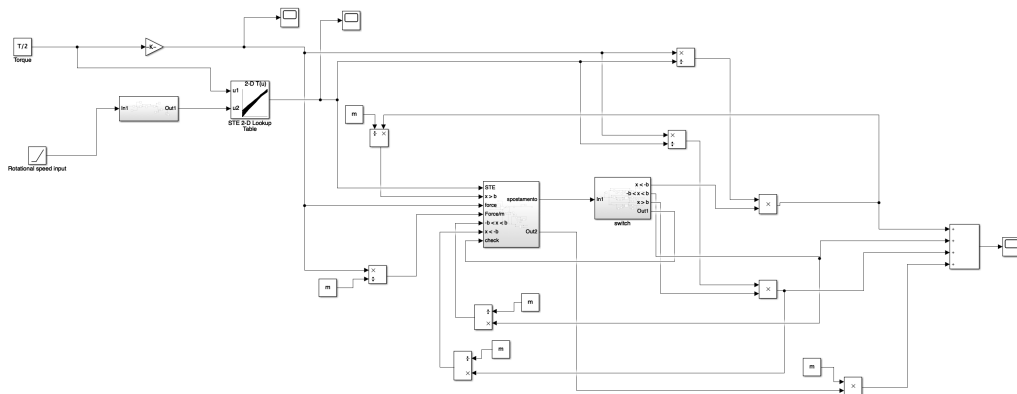


Figure 23: Simulink model

The complete Simulink model is reported above; as we can see the signal starts from the two only inputs of the system, torque T expressed by a constant source and speed expressed by a ramp, increasing from 0 to the final value with a designated increasing rate as we can see in Figure 24 that represent ramps settings.

Passing through several subsystems that will be studied in next paragraph, the signal comes to the final scope that represents the dynamic force between the two gears and which graphic result is represented in Figure 25; this block will enable users to graphically see the behaviour of the dynamic force plotted in function of time, that for these simulations has been stated at 8.44 seconds, in order to be able to compare results with experimental results and other older thesis works.

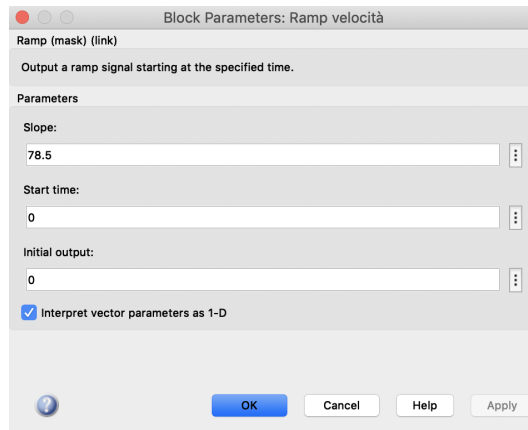


Figure 24: Ramp settings window

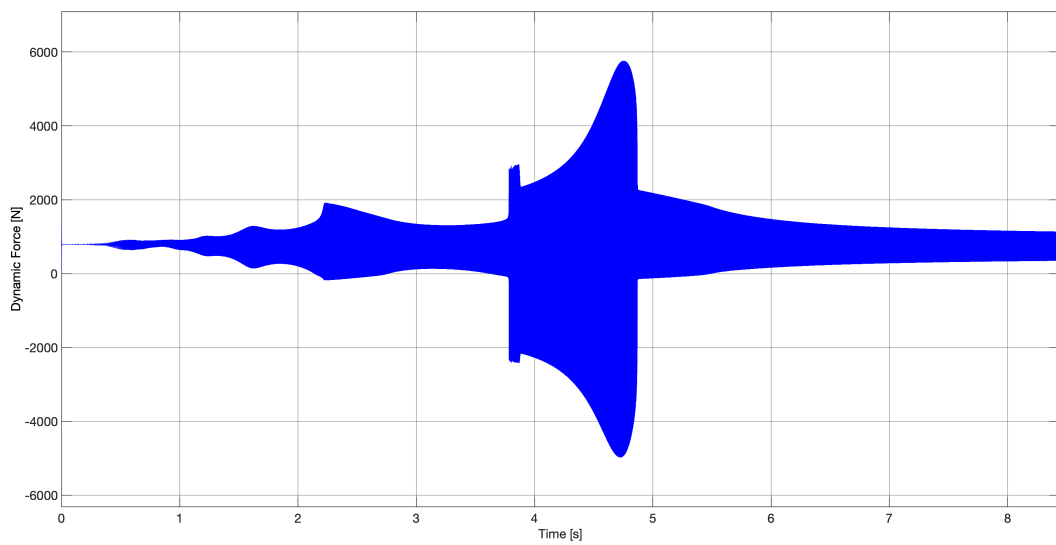


Figure 25: Example of output of a scope block

Many other parameters are also monitored all along the signal path in the overall system; by mean of several scopes we can obtain graphical representations of displacements of gear teeth, rotational speed, STE many other parameters such as contribution of damping and stiffness evaluation.

2.2 Analysis and purpose of the various subsystems

In this part all the subsystems present in the model are explained in their architecture, operation and main tasks; starting from the beginning of the signal path, the torque and speed inputs, and going through the model till the final output.

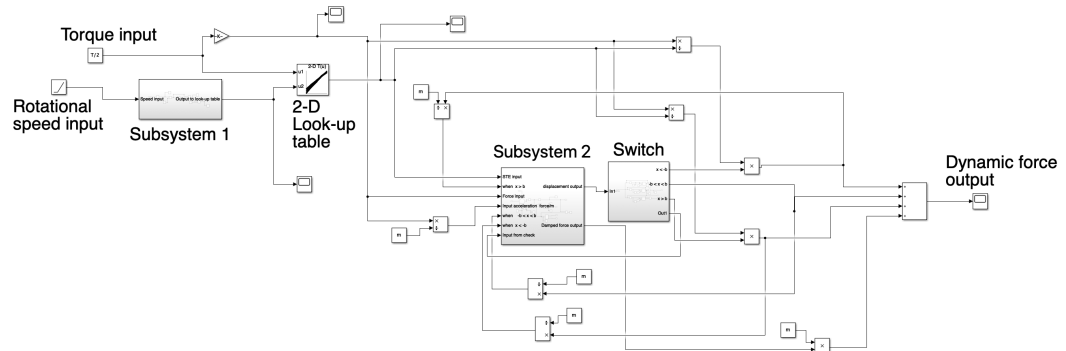


Figure 26: Subsystem division of complete model

2.2.1 Subsystem 1 and STE calculation

First subsystem we encounter in the signal path was created to compute data to feed the 2D look-up table that follows the subsystem in the scheme, in order to calculate STE.

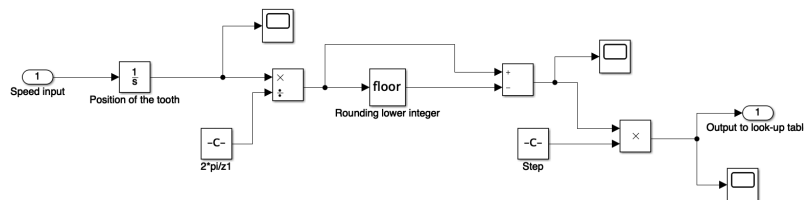


Figure 27: Subsystem 1

This subsystem has only one input that is the ramp source for the rotational speed, expressed in rad/s, and one single output. As we can see, we first

integrate the rotational speed to calculate the position of the teeth of the gear, after that , with floor function, we subtract the lower integer and evaluate exactly where we are in the gap between the two teeth. With some scopes blocks every value is monitored all along the process as in every other subsystem of the model.

After multiplying the result just obtained by the step we are able to exit the first subsystem and enter the look-up table reported below knowing where exactly the position of the tooth is in respect to the backlash present between two gear teeth. The look.up table takes as input the value just calculated and the value of torque given as input by the constant source block and, with data interpolation, it is able to calculate the STE that will be its only output.

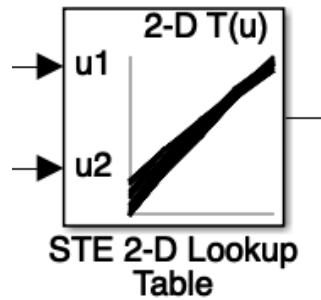


Figure 28: 2-D Lookup Table

Static transmission error will be fundamental to go on with calculations according to the theoretical models explained before in the introduction. Obtained the STE and the input force, that is calculated integrating the input torque, we can now enter the second big subsystem.

In the following figures (Figure 29, Figure 30 and Figure 31) are reported the main settings used to make the look-up table suitable for this task:

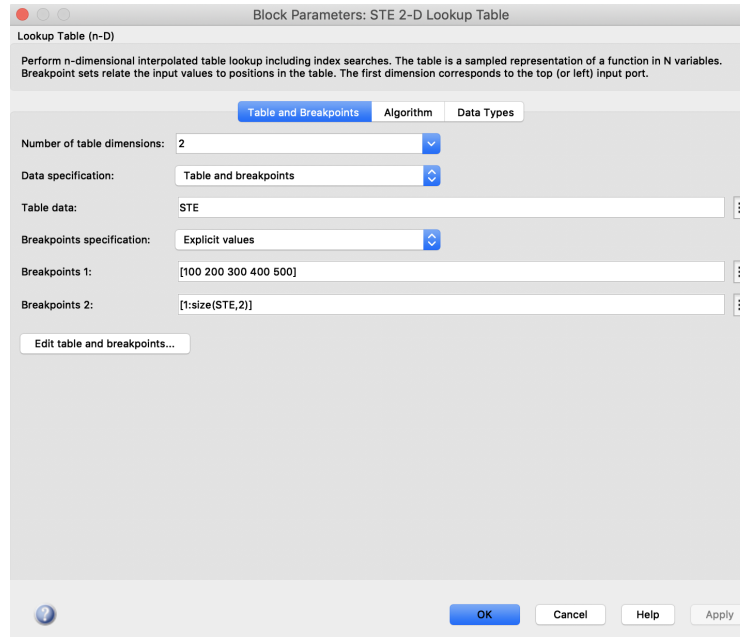


Figure 29: Look-up table parameters panel 1

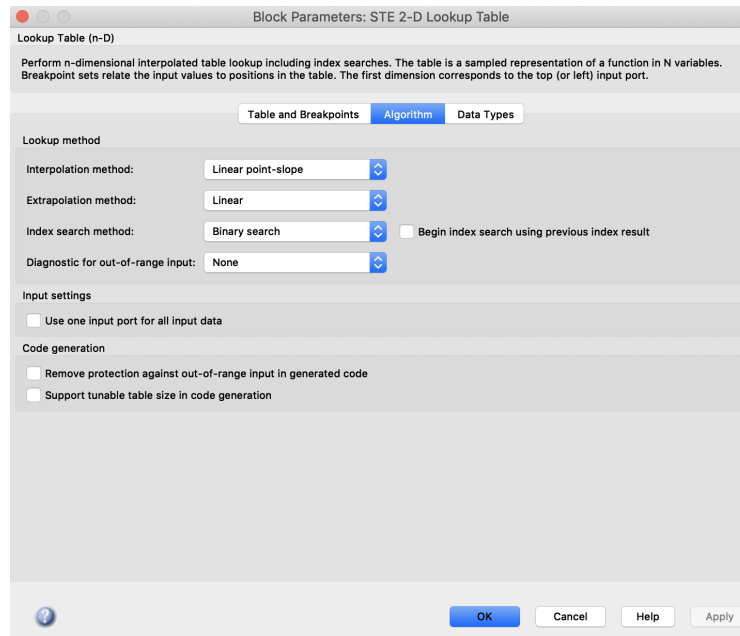


Figure 30: Look-up table parameters panel 2

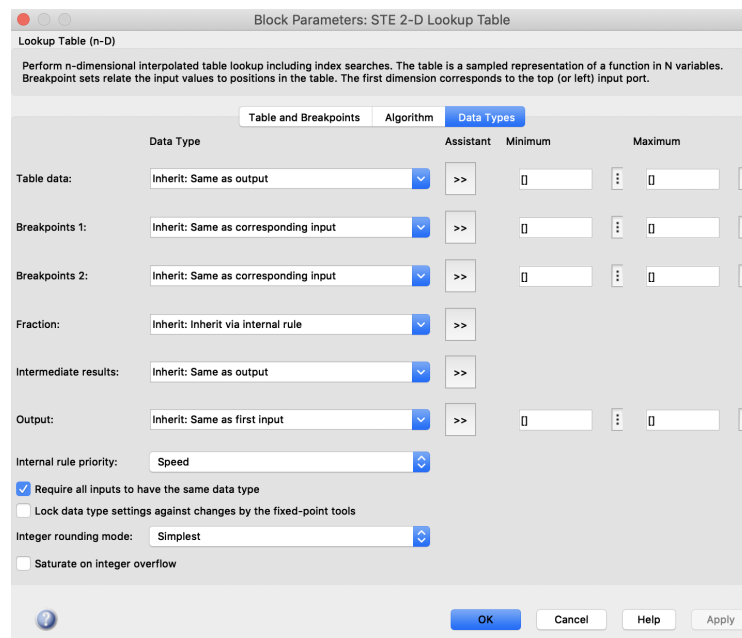


Figure 31: Look-up table parameters panel 3

2.2.2 Subsystem 2

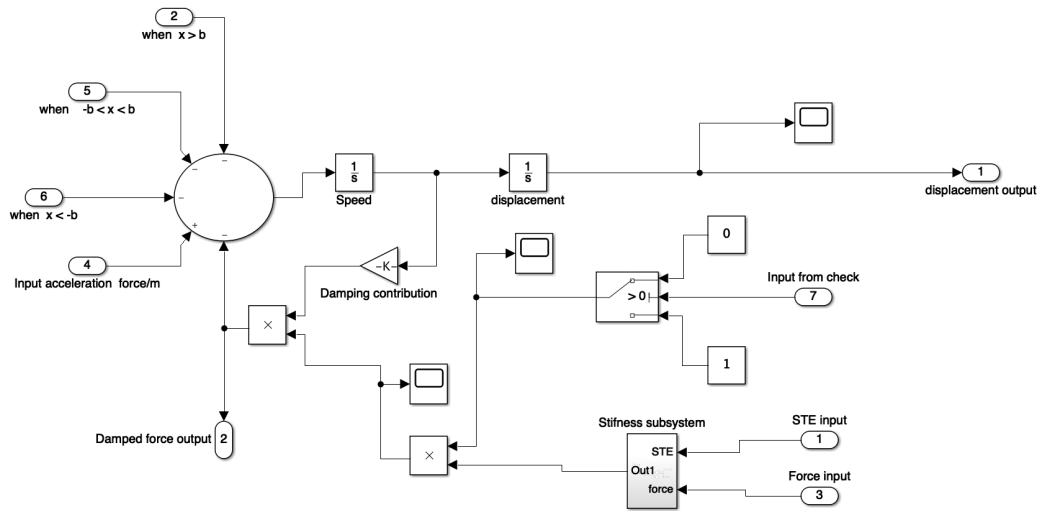


Figure 32: Subsystem 2

This subsystem has the goal of evaluating the displacement of the gear tooth by a double integration, but also taking into account the contribution of damping and the variation of stiffness. Looking at the beginning of the signal path of the subsystem we can see that there are several inputs that are coming from a switch placed after the subsystem itself that will be explained in details a little later on. In a few words this switch can evaluate where the displacement of the tooth is located in respect to the backlash and different paths, that will undergo different considerations and calculations, are switched depending on that position.

In general, the signals entering the subsystem are an acceleration expressed as the force divided by the mass value of the gear (input 4) and the contribution depending from the tooth displacement (just one of the three inputs 2, 5 or 6 depending on the value of the displacement).

The acceleration is integrated once to obtain the instantaneous speed and then another time to evaluate the displacement that will exit the subsystem in "output 1" and go on the the switch subsystem that we can see in details in next section.

In switch subsystem the position of the gear tooth in respect to backlash is evaluated; Figure 33 explains the three sections in which position is divided. The differentiation will establish three much different cases: in the first one we have displacement of the tooth bigger than the backlash, it means that

the gears in this case are in a situation of total grip, so we will enter again Subsystem 2 with a positive contribution to calculate the final dynamic force.

The second case is represented by the displacement in between the values of backlash, this case expresses the case of lack of contact between teeth of the two gears because the tooth will be in between the other meshing teeth without exercising any force on them. In this case in fact the signal path comes back to Subsystem 2 with a null force value.

Last case is represented by a displacement mathematically out of the backlash interval in the negative sense, it means that the gear tooth is in grip with the other meshing one, but with the two faces in contact will be the opposite that the one in the first case and so also the force imposed by the rotating gear will be the opposite and so will be the rotation verse too. In this case the signal goes back to Subsystem 2 giving a negative contribution to the final dynamic force calculation.

This last two implementation that consider the case in which we don't have the perfect and constant contact and grip of the two gears are very important to give the model a more realistic functioning and are fundamental to implement the case of torque inversion in the overall system.

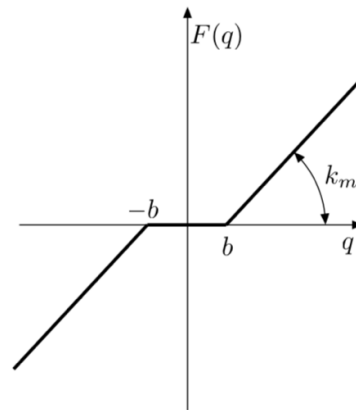


Figure 33: Non linear elastic force of teeth

Going on with the analysis of the subsystem we can see that after the first integration the value of the instantaneous speed is taken and multiplied by the damping factor and the contribution of stiffness to calculate the contribution of dynamic force that is influenced by damping; this contribution is then added negatively back to the input to take into account its effect also on displacements evaluated immediately after and with output 2 it is added to the other contributions of the force to calculate its final value.

Going to the last part of this subsystem we observe that we have a further subsystem inside this one, that is the one in charge of calculating the values of stiffness of the teeth; it is reported in Figure 59.

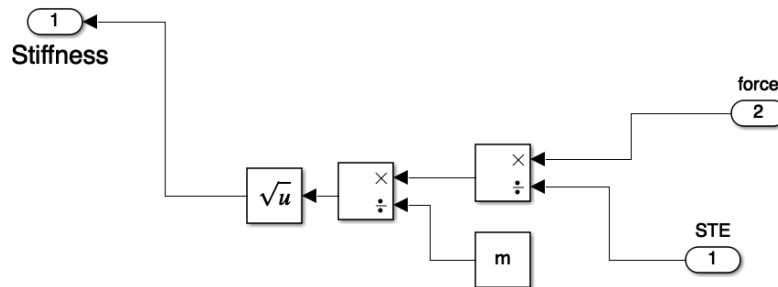


Figure 34: Stiffness evaluating subsystem

In a more detailed look for what regards the calculation of the stiffness we have as input the STE and the force applied to the gear as we can see in Figure 59. Dividing the force by the STE and dividing again by the gear mass we obtain the square value of the stiffness, that after being reduced by the square root block is introduced in Subsystem 2 to influence the calculation of dynamic force.

2.2.3 Switch

In Figure 35 we can see the switch subsystem used to separate the three different paths depending on the value of displacement respect to the backlash interval.

This task has been accomplished taking as input the tooth displacement from the previous subsystem and using signal routing blocks shown down here in Figure 36 and Figure 38 to evaluate the input value and distribute it in the different cases.

The first one is a block that compares the input signal with a constant chosen by the user (in this particular case I used one for a positive backlash check and another one in a separate branch for a negative backlash check using in one the value of backlash "b"and in the second one "-b"); this block uses boolean logic, it gives as a result 1 if the statement made in the block (which the user has to specify in advance in the block settings as shown in Figure 37) is true, otherwise it gives a 0.

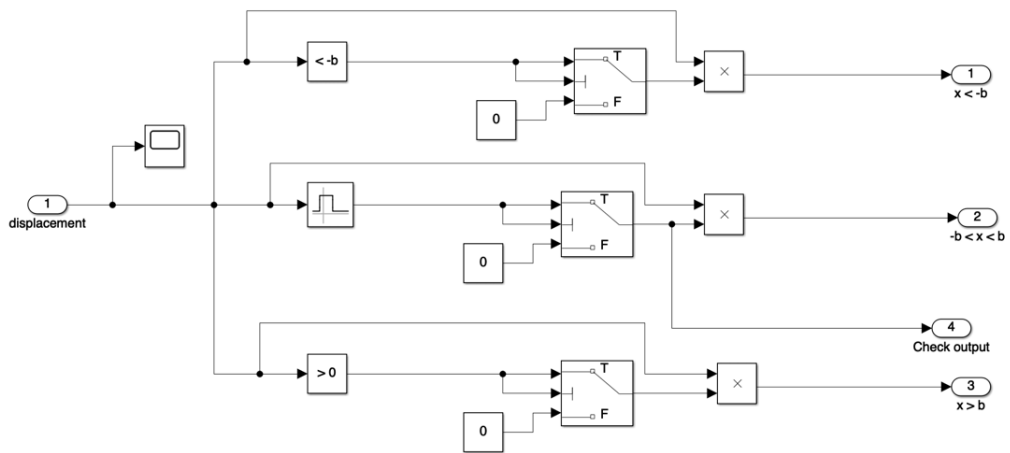


Figure 35: Switch subsystem

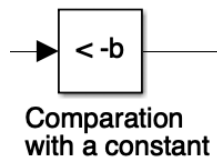


Figure 36: Comparison to constant block

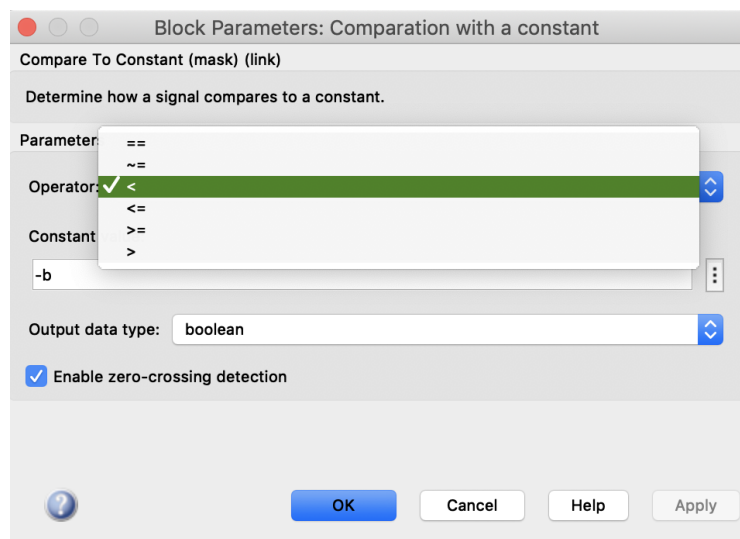


Figure 37: Comparison to constant user panel

In the mid branch of Figure 35 another signal routing block is used, the interval test block. Its function is to check if the input value enters in an interval specified by the user in the block panel (Figure 38) and as the block explained before, give results of 1 or 0 for true or false results.

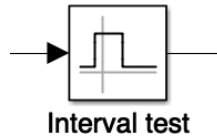


Figure 38: Interval test block

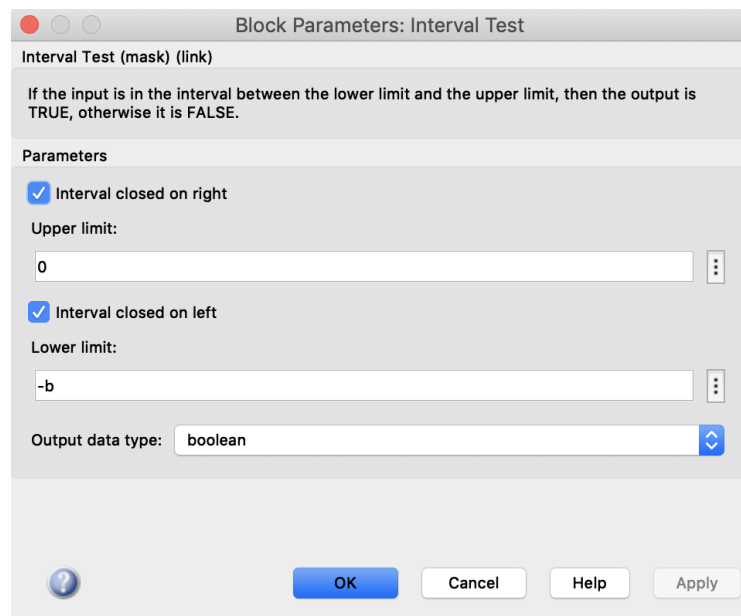


Figure 39: Interval test block panel

Going on in the signal path every one of the three branches present a switch block (Figure 40); this block routes the signal in a way that if the statement imposed in the block panel is true, the original signal will go on in the path, otherwise if the statement isn't true the signal will exit the block to a constant, that in this case I chose to be zero.

After all this routing functions, in all the three branches the result is multiplied by the original value of the displacement. The logic behind this subsystem is that with the routing system I would have just one of the three branches having a value of 1 at a time when the other two would be null; the only one different from zero would be the one interested by the backlash check. Multiplying the non null branch by the original displacement value I will have, at the output of

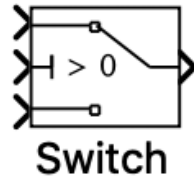


Figure 40: Switch block

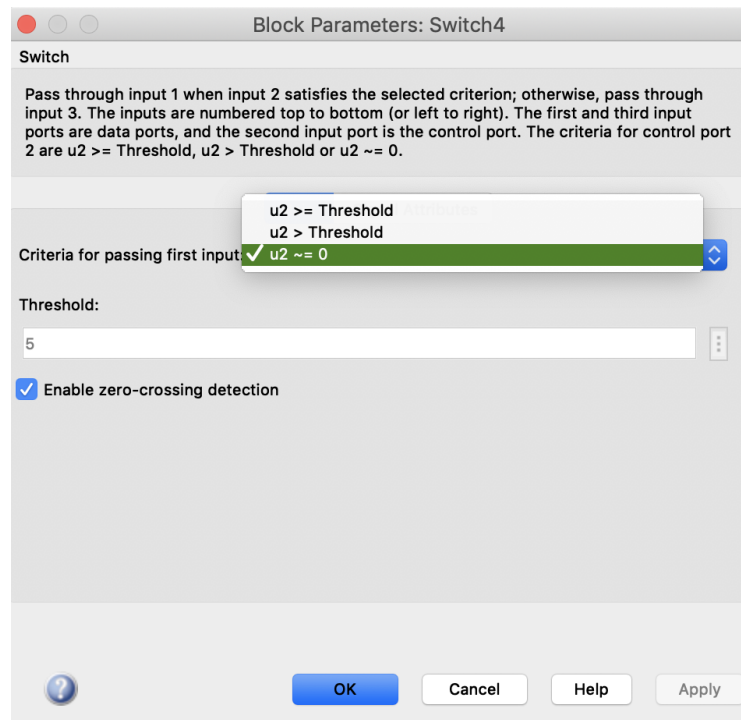


Figure 41: Switch block panel

this subsystem, the exact value of displacement in the branch that represents the case of study, while in the other two the output value will be zero.

This permits to have just one path of the three re-entering subsystem 2 at a time, re-inserting in calculation the value of displacement of the right "case" we need to calculate, as explained before.

2.2.4 Final operations and output

In the last part of the model every contribution calculated before is added together in a single signal, that will represent the final value of the dynamic force acting on gears we wanted to calculate.

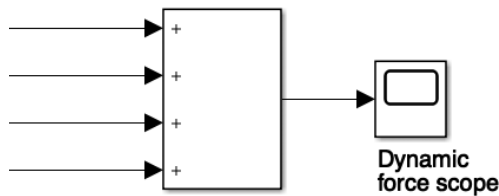


Figure 42: Final output of the model

All contributes of different forces are grouped by a sum block and then all together go on in a scope block that will give us the graphic representation of the dynamic force; the contributions include non damped force, damped force, the force calculated when there's no contact between gear teeth and the force imposed when gears are in contact in an inverse sense of rotation or when they vibrate or bounce against each other.

3 Torque inversion

After successfully modelling a system able to calculate the dynamic force acting on two meshing gears a very important function has been implemented to the model; the ability to recognise if a negative torque is applied to the geared wheels, that will begin to spin in the opposite direction.

In this chapter will be explained the main steps I've gone through to implement the function of detecting and dealing with a negative torque inside the complete model explained before.

The main purpose of this addition is to give the system the ability to react to every input that it can be fed with, reacting to negative torque values evaluating the dynamic force and every other parameter that was able to compute in the previous version explained in chapter 2.

3.1 Implementation of the model

The most limiting factor of this implementation was the integration and the calculation using a negative input using the same signal path and the same algorithm than the previous model; Simulink in fact doesn't allow this type of calculation and it made impossible for me to calculate all the parameters in the same exact way in the two cases of torque input.

The problem has been avoided separating the two different paths, but switching the one that is not in use off while the torque inversion happens for keeping the model as light as possible and as fast as possible to run not making extra non needed calculations.

This task has been accomplished placing a torque switch selector right after the torque input, that is able to evaluate the torque and recognize when it goes down to zero and when it inverts; then the path is divided in two, the two contributions resulting from positive and negative torque are separately calculated and added one another at the end of the system.

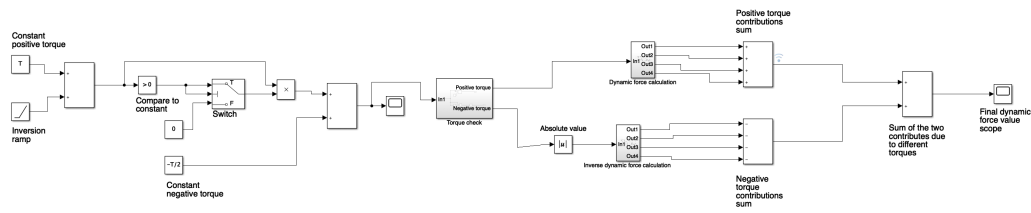


Figure 43: Torque inversion model

Subsystems used to evaluate the dynamic force are very similar to the one presented in the previous model, with the difference that in the negative torque branch both the displacements and the dynamic force are calculated putting the negative torque in absolute value and then considering its contribution opposite to the standard torque one. With this trick we can avoid the problem of negative input integral calculations into the model.

3.1.1 Input torque determination

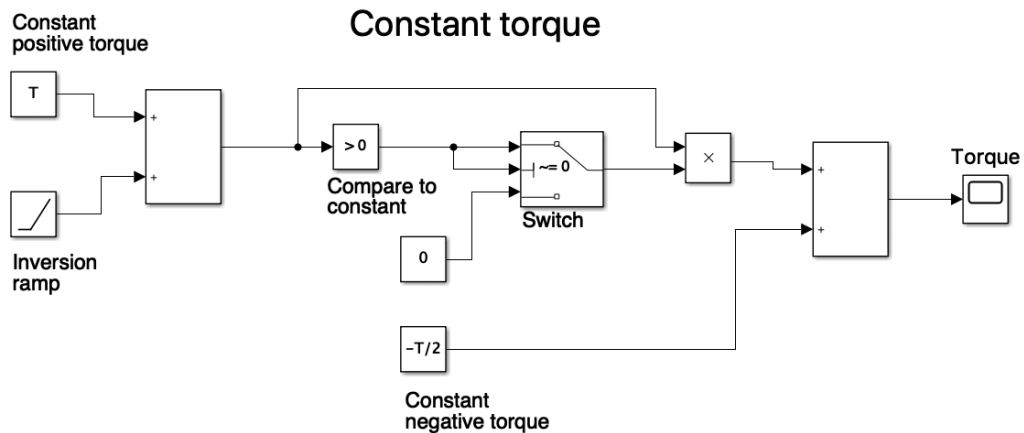


Figure 44: Constant torque input blocks

Starting from the beginning of the signal path we have the torque input and immediately from taking a look at the scheme of the model we can see that it differs from the previous one by many elements.

The two input in the simulations are again torque and rotational speed, but while in the previous model the rotational speed was represented by a ramp starting from zero and growing with time, in this newer system speed is kept constant; what is varying during simulation is only the torque.

The constant block that I used to create the torque input has been replaced by a series of blocks that enabled me to simulate a constant torque that, at a certain moment that can be programmed, starts sinking very rapidly to zero and even lower and, when it reaches the opposite value, it becomes constant again (this time it is negative).

The blocks I used to achieve this function are quite simple but they have a specific logic behind their placement; I started from a constant input block giving a constant torque value starting at the beginning of the simulation. At a certain moment, a negative and very strong ramp signal is added to the constant input mentioned before, starting to lower it very rapidly; the moment in which the ramp turns on is considered to be the start of the torque inversion and its timing is chosen by the user in the panel window of the ramp block.

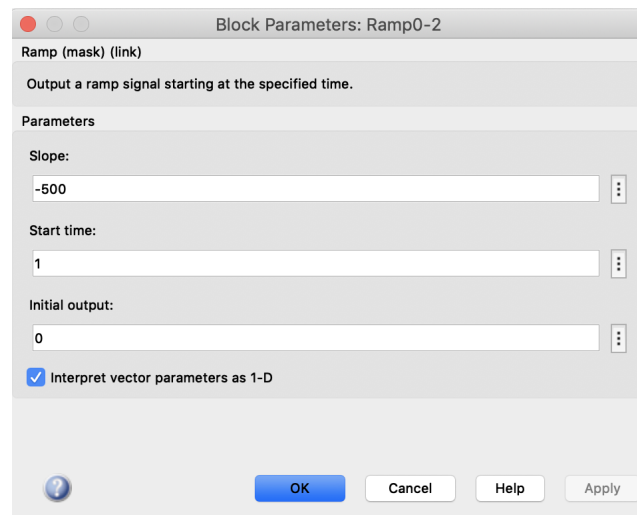


Figure 45: Inversion ramp block panel

The ramp parameters are set deciding at what time we want torque inversion, imposing a ramp start time, and how steep we want the the decrease to be using the slope value; the more gently the torque goes down, the more we can observe the phenoms taking place when torque starts decreasing an goes negative causing the change of the rotation verse of the two meshing gears. In the case reported in Figure 45 the torque inversion is quite rapid and it is set to begin at 1s from the simulation start.

Going on in the signal path we can see that two routing blocks are presents, a compare to constant and a switch block; this two coupled permitted me to check whenever the torque value reaches the null value comparing the torque value from the two inputs explained before to a constant 0 and then make a check with the switch block: if the signal coming from the previous block is 1,

this value will go on and after the multiplication block we will have the original torque value whenever it is positive, otherwise it will exit the switch block to the constant zero remaining null.

After the signal routing section we have the last block that composes the torque input system, it is a constant block that will enable us to have, after the initial constant torque and the rapid descending of it, a value of torque that it is constant, equal to the previous one and negative. A scope block is put at the end of this part of the model for monitoring the torque value, and example of the result that can be obtained is reported just below:

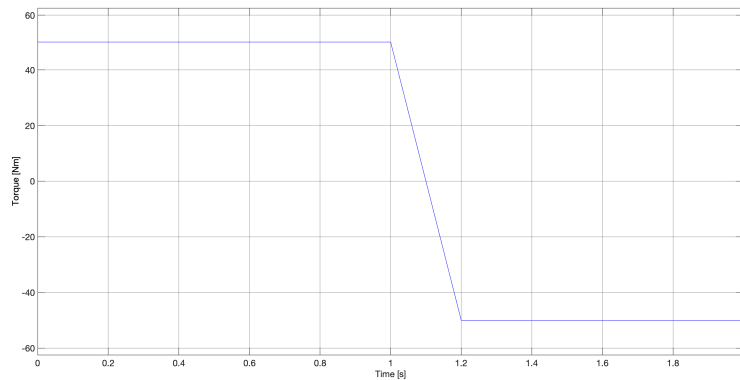


Figure 46: Torque input result

I designed also another way to define input torque, different from the one we have just seen, that permits to have instead of a constant torque before and after the inversion, an increasing torque starting from 0 and, after the inversion, a negatively increasing torque till the desired value. The Simulink scheme is shown here:

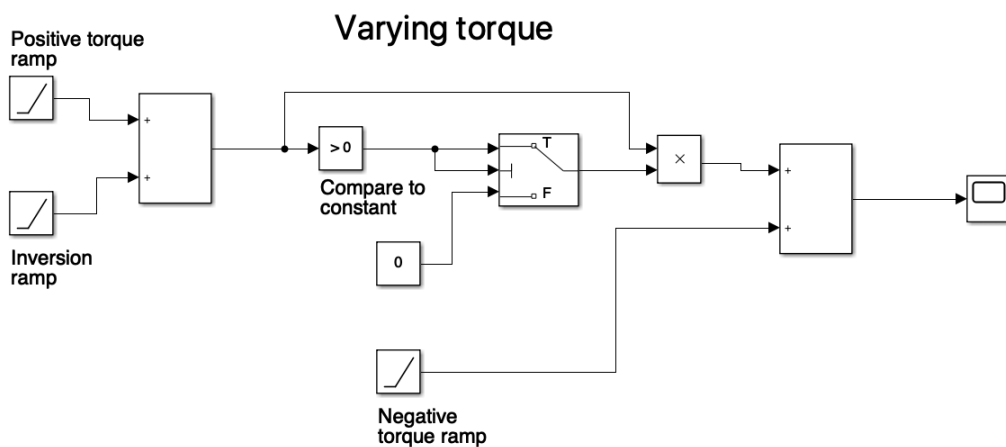


Figure 47: Varying torque input blocks

The working principle is the same than before, but this time instead of the constant blocks giving torque values, there are other ramps that represent the increasing torque in the first one, and the negative increasing one in the second. The ramp responsible of the inversion remains the same and the routing sections also remains unchanged.

Also in this case a scope is put at the end of this section, before the signal enters the torque switch to be divided in two paths.

An example of torque signal obtainable with this system is showed below:

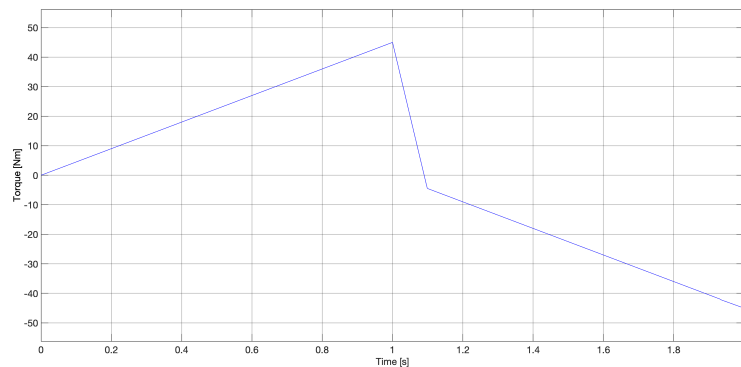


Figure 48: Torque input result with ramp blocks

After the input torque determination, the signal proceeds to the torque switch selector to be divided into two branches.

3.1.2 Torque switch selector

To divide the signal path in two parts depending on the input torque they are receiving I created a subsystem that is able to detect the value of torque, analyze if it is higher, lower or equal to zero and direct it as a consequence.

As we can see in Figure 49 the subsystem takes the torque as input and sends it to a switch block, that will make the signal pass through if torque is higher or equal to zero, and to a comparator to a constant block, that will make the signal go on if the torque is lower than zero. The two routing blocks will reduce the signal to zero if the statement assigned to them isn't correct.

I didn't use the same routing function on both cases of torque because switch block doesn't allow be set up with a detection of values lower than zero, so I had to use the comparator to constant block in case of negative torque. The output of that branch is multiplied by the torque itself because we have to remember

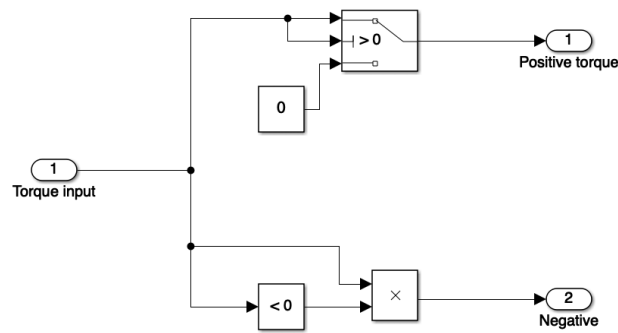


Figure 49: Torque switch selector

that comparator blocks use boolean logic so without the multiplication the only output of that block would be 0 or 1.

The main good characteristic of this way to separate the two branches is the fact that using boolean logic paired with the switch Simulink block, if first branch isn't in use, the program won't have to make all the calculation of that branch to give a null result but the signal immediately exit to a constant zero, saving computing time for the program to go on in simulation; in a shorter way, if torque is negative, positive branch will just be shut off and vice versa. With this trick, the model remains quite fast to run with not much difference in comparison with the previous one that doesn't include torque detection.

3.1.3 Dynamic force calculation - positive torque

Coming out of the torque switch selector the signal path is divided in two separated branches, one for positive and one for negative torque.

The branch coming out of the switch when we have a still positive torque value will proceed in dynamic force calculation, the calculation has the same exact steps that we have seen to calculate the dynamic force in the previous model without torque inversion, so the final result will be the sum of all the components of force due to damped contribution, non damped contribution, non contact and reverse contact forces.

So for this branch there haven't been many modifications a part from the input data, in the detail of the force calculation subsystem we can see the changing of the input rotational speed that in this case is represented by a constant block expressing speed in rad/s.

For the rest of the subsystem no more changes have been done so it follows the same architecture and operation system and rules that the one explained before for dynamic force calculation; subsystem 1, subsystem 2 and the switch are also the exact same subsystem that the other model.

3.1.4 Dynamic force calculation - negative torque

The dynamic force calculation related to the branch coming out of the torque switch with negative torque is a little bit different from the positive one.

First of all we have to point that Simulink with this type of operations and calculations won't accept a negative value as an input, otherwise it will give several errors and whenever a simulation will be started, it will interrupt giving random values to the final result.

To avoid this complication, the signal path that represents a negative torque input is inserted in the subsystem in charge of calculating its contribute to the dynamic force with the use of an absolute value Simulink block, this way the force can be computed at the end of the calculations. This contribute of dynamic force however is related to a mathematically negative torque, that represents a torque applied in the opposite sense of rotation than before, so at the end the contribution of this force will be opposite from the one calculated in the previous sense of rotation (expressed by positive torque).

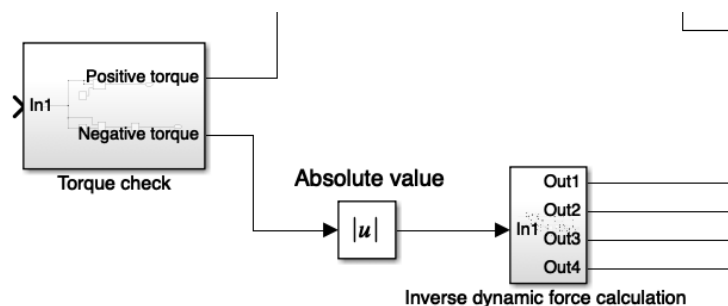


Figure 52: Negative dynamic force contribution subsystem

3.1.5 Final section and overall dynamic force

In the final section the two final contributes of the dynamic force of the two different branches come together; as already said the force component coming from a positive torque will be positive in the convention of positive sense

of rotation chosen at the beginning, while the other contribute will be the opposite.

Simple mathematical addition block takes care of the sum of the two contributes, after that all single contributes of damped, non damped, contact less and reverse contact of every branch are joint together.

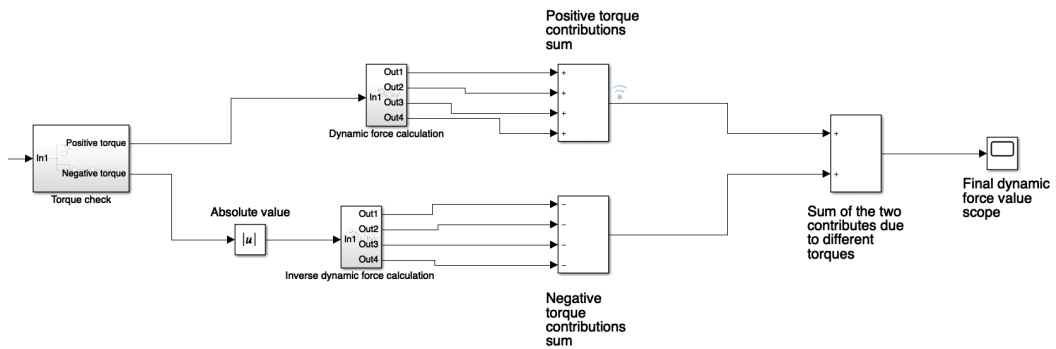


Figure 53: Final operations to get the overall dynamic force value

This way we also have a method to evaluate the dynamic force of a two gears meshing system regardless the input torque or speed is given. We don't bother having positive, negative, growing or shrinking torque or speed, the system is autonomous in detecting what kind of input it is receiving and how to deal with it in order to accomplish the task it has been designed for.

4 Simulations

Many simulations have been made to evaluate the main parameters of the gears in exam, in particular two main type of simulations are reported in this work: simulations with and without torque inversion as well as all the result of all the simulation run.

4.1 Simulations without torque inversion

First of all I've done simulations on the simpler model without torque inversion, this simulations had the task to evaluate dynamic forces acting on gears and their behaviour, in simulations' results we will be able to see how the dynamic force changes with rotational speed, where characteristic frequencies are present and how it affects the stress on gears.

In the following chapter I explain the procedure I followed to make all this calculations and the parameters I set for making these simulations as reliable as possible.

4.1.1 Simulations settings

After modelling the entire Simulink system various simulations have been done to analyze the behaviour of the meshing gear in exam.

Starting from the setting of basic parameter of the two gears we defined them with this parameters:

- Mass $m=0.5275$ Kg
- Number of teeth $z_1=z_2=28$
- Backlash $b=2.5 \times 10^{-5}$ m
- Module=0.005
- Inertia moment $J_1=J_2=0.042$ Kgm^2
- Damping factor $\zeta=0.08$

For what regards the first input value to insert in the model, the torque, it has been chosen a constant value of 50Nm expressed by a single constant Simulink block since this model has been run without torque inversion.

Other only input is rotational speed and for this test it has been set as a ramp value, starting from zero and growing with a speed of 78.5rad/s per second, overall simulation time has been set at 8.44 seconds in order to match with other simulations done before me by other students. This simulation time has been chosen also because it is quite short for the program to compute all the calculations, but according to torque and speed values it is enough to observe a lot of phenomenons that take place in the meshing of this two gears.

Looking at the list of gear parameters we can see at the end the damping factor zeta; this parameter express the damping effect of the lubrication oil film that circulates inside the system and that will damp the contact between gear teeth of different geared wheels.

This value of zeta=0.08 has been taken from literature, it represent an experimental evaluated value so, for these simulations, it has been left as it is in order to study the general behaviour of the system and how it compares to an ideal theoretical one. Beside that in further simulations we will observe that a lower value will permit us to observe and study more phenom presents in gears behaviour.

4.1.2 Simulink settings

The program settings for running this type of simulation is a little bit different than standard; the main parameter that had to be changed was the solver itself, from the auto mode it has been turned into ode45. Also the step size in analyzing the system has been changed, it has lowered to $1e^{-6}$ from its standard automated value. It simply represent how small the time interval of calculation will be, in this case 1s is divided in 10^6 segments.

To define a proper step size I didn't use any particular method, I just tried to lower it step by step until I reached a value that permitted to analyze graphs coming out of scope blocks in a clear way. Also the zero crossing options where changed, turning from "non adactive" to "adactive". At last the function "automatically handle rate transition for data transfer" has been activated.

All this modification can be done entering the configuration parameters window of Simulink.

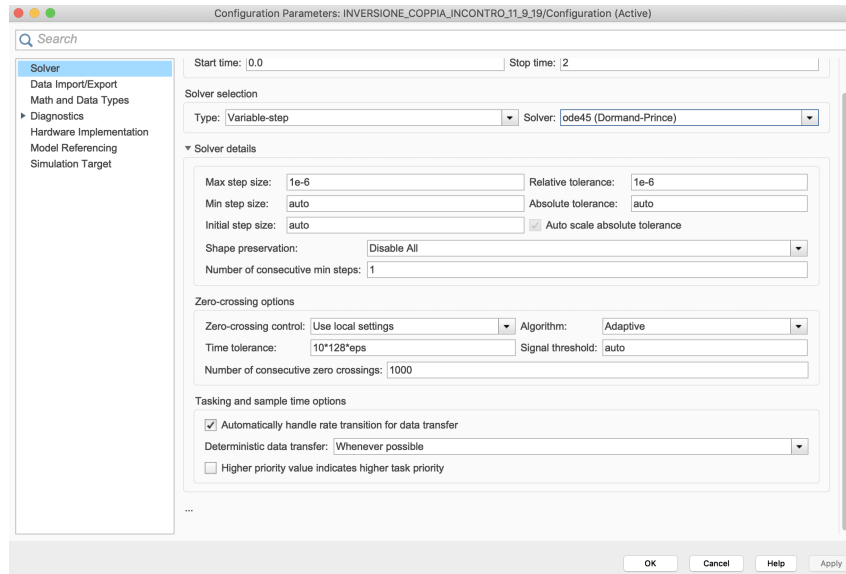


Figure 54: Simulink configuration parameters window

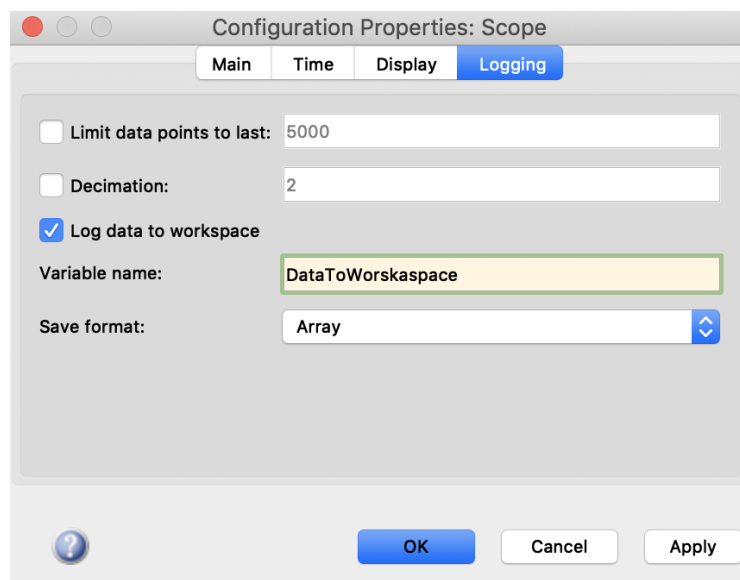


Figure 55: Configuration properties of scope blocks

Another parameter I tweaked before starting the batch of simulations is related to scope blocks; entering the configurations properties, clicking on the "view" icon, and entering the "logging" section, we can save the data that the scope block is receiving and log it as an array of values to the Matlab workspace. With this fundamental function we can import data obtained by calculations from Simulink to Matlab; having these data in Matlab means that they will be easier to turn into plots that are much more modular than Simulink ones, being able to manipulate plots in a much easier way to understand and to present graphically.

Any other Simulink setting has been left stock as it is when starting the program.

4.1.3 Simulations results

After setting everything up all the simulations had to be ran; in this section the main results of the simulations I run are shown.

The final results I was more interested in were the gear teeth displacements and the dynamic force between the meshing gears; however many other parameters are monitored during simulations in order to have as much information as possible and also to check if results are coherent with meshing theory.

Starting from the beginning of the model the first element to be monitored is the value entering the 2-D lookup table that will calculate STE, remembering that it express the instantaneous position occupied between two subsequent gear teeth and its values mustn't be higher that the step (so not higher than 0.041mm) and lower than zero. The value coming from a scope put at the output of Subsystem 1 shows us this result:

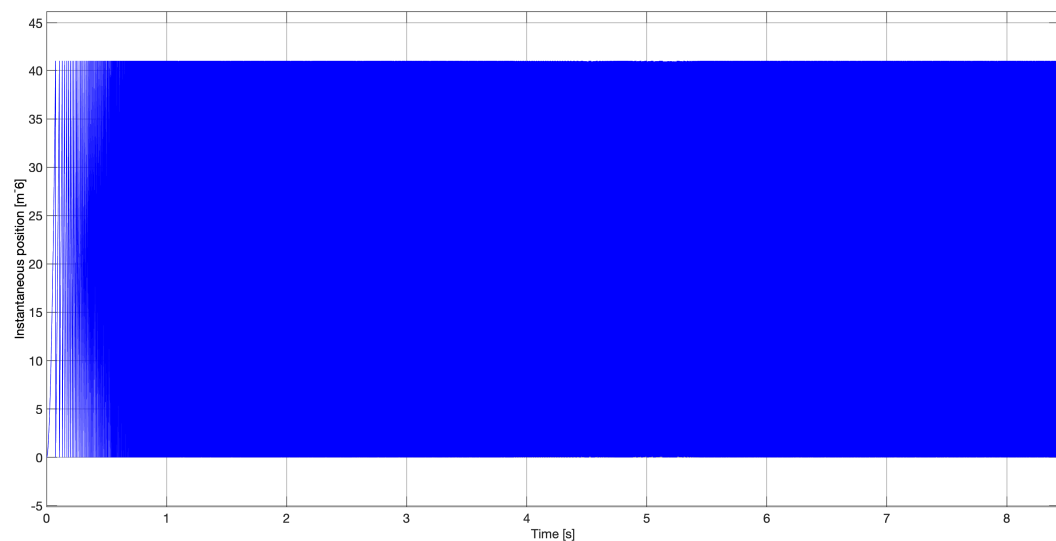


Figure 56: Data entering the 2-D lookup table representing the instantaneous position between gear teeth

After that, going through the lookup table we are able to see how STE turns out to be and it is reported in Figure 57

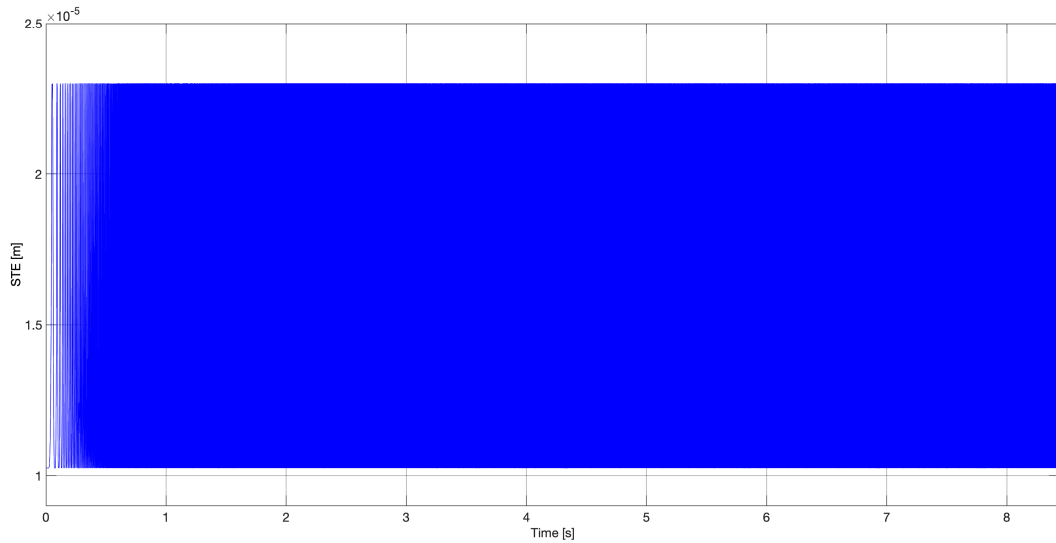


Figure 57: Static transmission error STE

Going on with the signal path explained in the previous chapters, we now have to face displacements and stiffness calculated inside Subsystem 2; gear teeth displacements are reported in Figure 58 and stiffness is reported in Figure 59

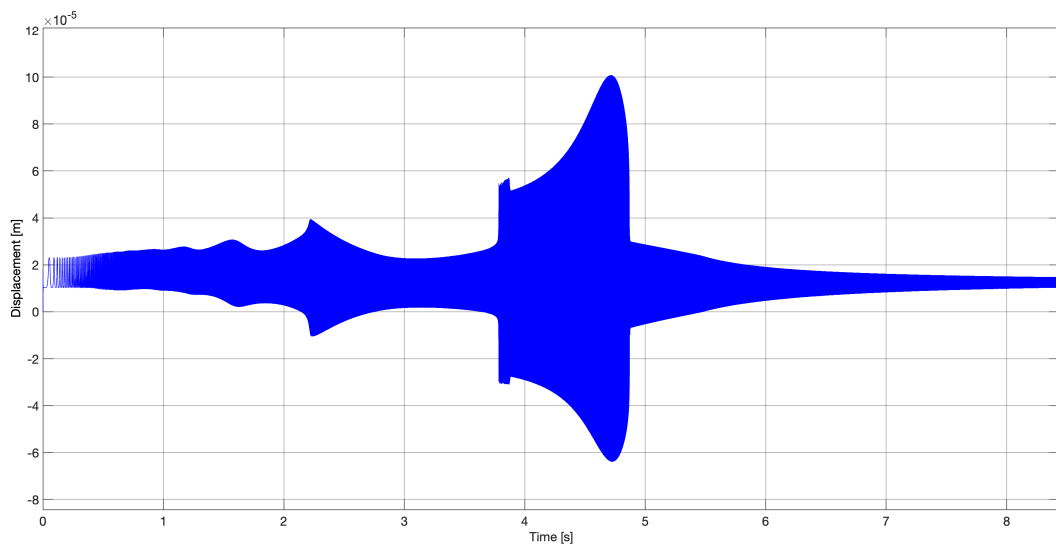


Figure 58: Displacements

With all this data the calculations of the various contribution of the dynamic force are possible and here are all the plots of the different contributions, starting from the damped force contribution in Figure 60.

Then we have the non-damped force contribution in Figure 61

Looking at those plots we can see how much damped contribution of force prevales on non damped one and how they have the same behaviour, confirmed by the behaviour of teeth displacements.

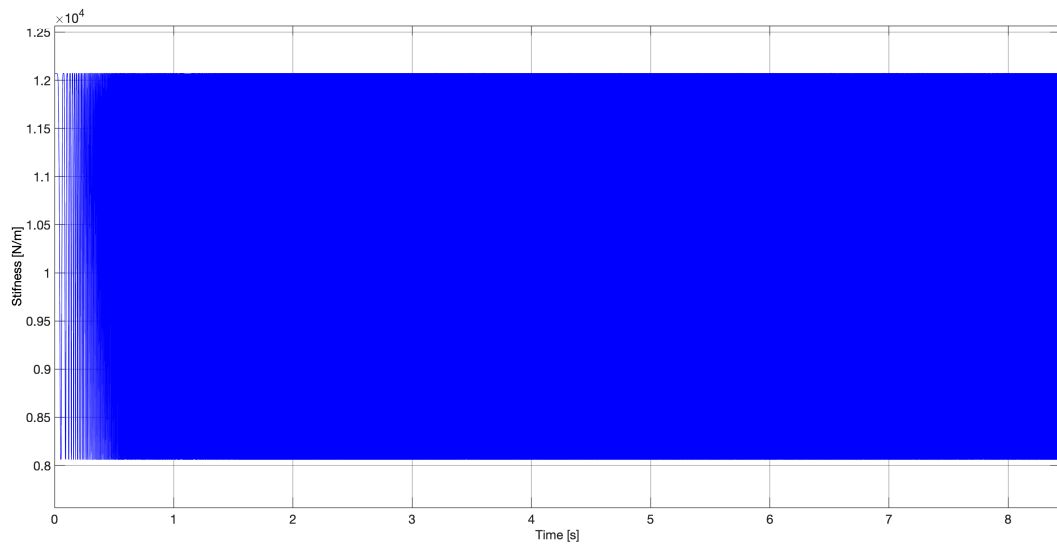


Figure 59: Calculated gear stiffness

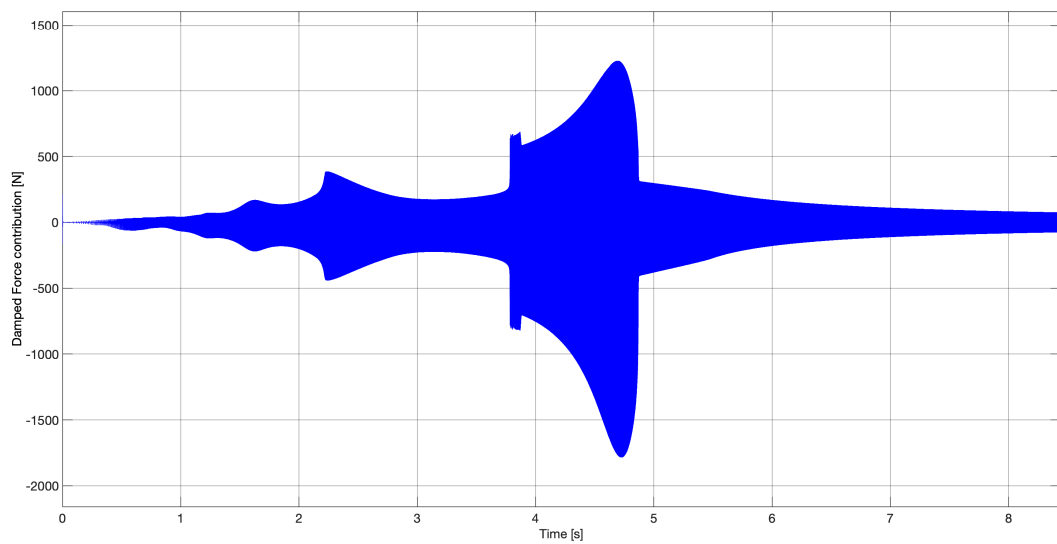


Figure 60: Damped force contribution

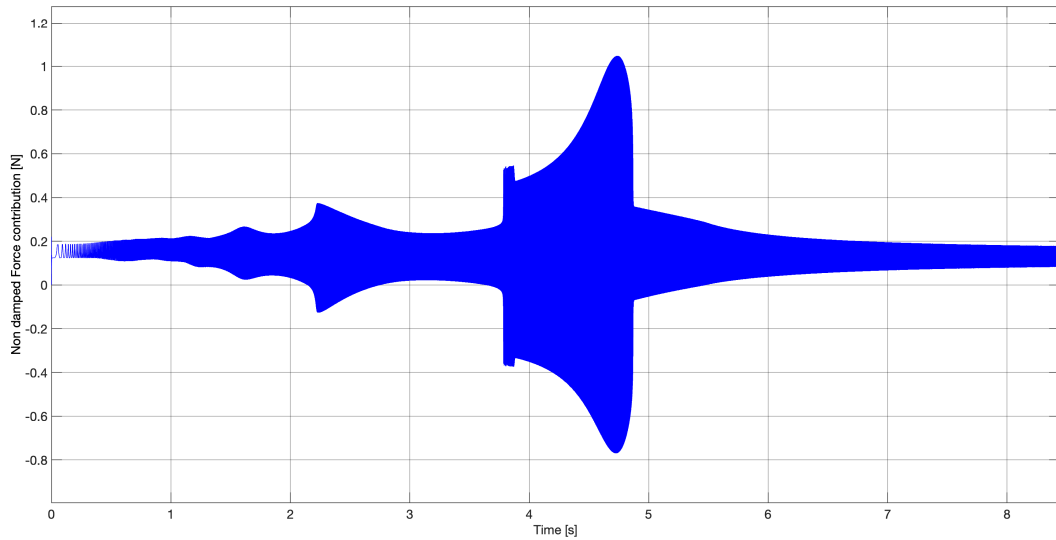


Figure 61: Non damped force contribution

At last the most important value is calculated and graphically reported, the overall dynamic force between the two meshing gears in Figure 62.

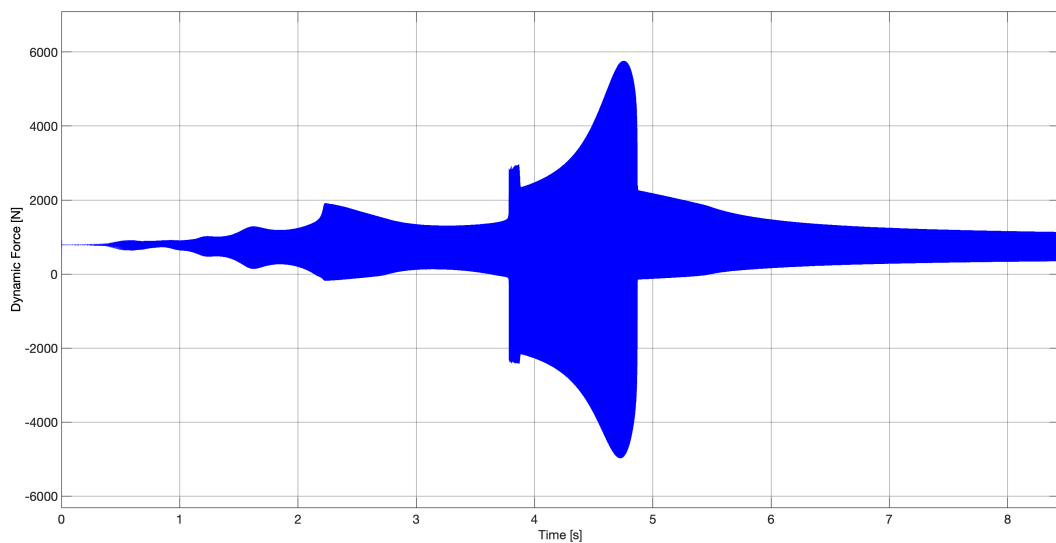


Figure 62: Overall dynamic force between meshing gears

A lot of things can be said regarding dynamic force's plot; first of all we can analyze the behavior of the force depending on time and so on rotational speed. As we know rotational speed is defined by a ramp block so it is strictly related to simulation time; at different times in the graph we can see peaks of dynamic force and in other we have segments in which the force is quite low and stabilized, this dependence must be translated in dependence between force and rotational speed.

At different speeds we can observe different behaviours from this last plot, starting at low speed we have low values of dynamic force with small oscillations until we reach approximately 1800 rpm (a little more than 2 seconds from the start of the simulation); here we observe quite a big oscillation in force value that will lower immediately after.

The biggest phenomenon present in this analysis is the jump phenomenon; a very high peak of force that takes place at around 3800 rpm (4.8 seconds from the start) that will bring major consequences of the system such as gear vibration, noise and irregularities in meshing. Immediately after the jump the force value will lower to a stable value and keep itself almost constant.

All this oscillation phenomenons are due to the characteristic frequencies of the system, to every frequency and so to every rotational speed value corresponds a peak of force, smaller or bigger depending on many factors, that will characterize this system; for example changing the damping coefficient value the value of the force peaks will change (higher force with lower damping and vice versa) but the speed at which the peak take place will remain the same. This will be the key to study torque inversion implementation and vibration of gears later on in this thesis.

Comparing the force values with displacements it is clear from the Figure 58 that at the highest peaks of dynamic force corresponds the highest peaks of displacements of gear teeth; this is a good sign of the correctness of the model presented and it makes everything more coherent with experimental calculations and theoretical studies.

This model at the end has turned to be very reliable and precise if compared to theoretical results and analysis, the behaviour of the parameters monitored managed to be the same expected from theoretical studies and experimental tests, giving us a very suitable platform to analyze gear pairs and their meshing with a fast and accurate model. But more implementation can be done to make its way of working more autonomous and some of them are the main topic of the next chapter.

4.2 Simulations with torque inversion

What I want to describe in this section is the method and the procedure I went through in order to make the system more autonomous in input detection and calculation; the model shown before in fact doesn't work if the input torque goes to zero and below, or in other words if gears stop and start rotating in the opposite direction. In the next lines the process to make the model more versatile are shown and simulations results are reported.

4.2.1 Simulations settings

Simulation settings were set very similar to the previous simulation ones with some exceptions; what remained unchanged are the geometrical and inertia parameters of the two gears, the mass and the number of teeth:

- Mass $m=0.5275$ Kg
- Number of teeth $z_1=z_2=28$
- Backlash $b=2.5 \times 10^{-5}$ m
- Module=0.005
- Inertia moment $J_1=J_2=0.042$ Kgm^2
- Damping factor $\zeta=0.034$

The damping factor is one of the most important differences between this model and the previous one, the higher value used before was intended only to study the behaviour of the force respect to the characteristic frequencies and that aspect won't change with damping parameter (force valued will change decreasing damping but the speed at which there will be jumps or resonances will remain the same).

For this study I employed a value of $\zeta=0.034$; I tested put some different valued between this and the previous one and this seems to me the best one to analyze this phenom.

As we will see in simulation results with this value of damping we are able to have classic functioning of the gears in the opposite rotation side, but also to detect vibration in gears when rotating at speed in which we have jumps of force values. With too low values of damping factor in this particular system we would have vibrations even with very low force or at the opposite with too

high values we won't have any vibration at all; both the two cases wouldn't be so coherent with a real practical usage.

Time length of the simulation has been lowered to 2 seconds, in order just to study the phenom of inversion; it was chosen to be long enough to observe the inversion but also the stabilization of the force after the application of the inverse torque without missing any phenom that could take place in the immediate instants after.

Also rotational speed has been changed, in this case simulations where done at different steps of constant speed, the values of speed where chosen looking at the dynamic force diagram of Figure 63. Following the conclusions of the previous chapter where I observed that to some specific rotational speeds this system presents resonances and force peaks, five different speeds where used in order to observe the phenom in every characteristic point of the diagram, going through low force, high force and where characteristic frequencies are presents.

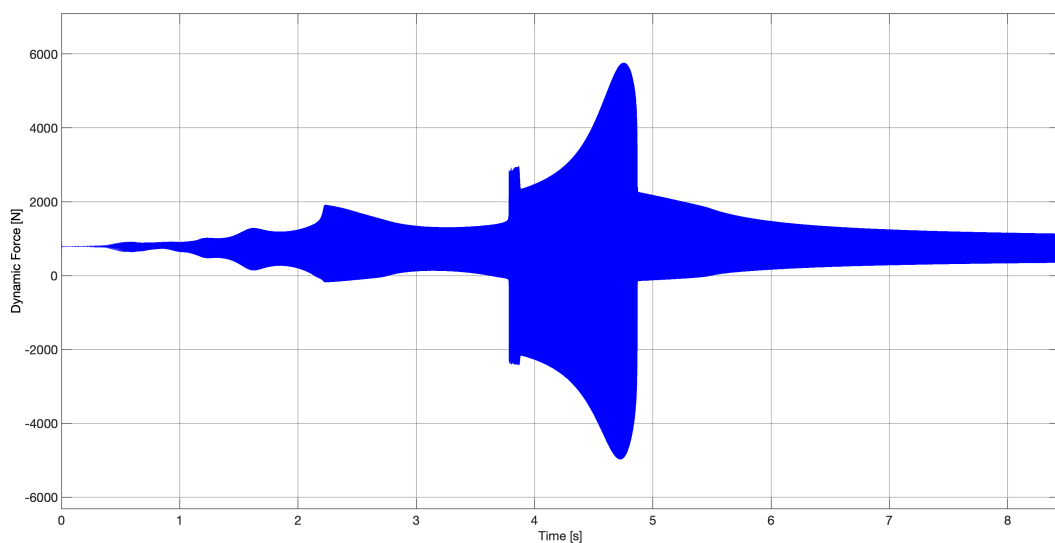


Figure 63: Dynamic force in function of time

In order to have more variety of results the rotational speeds chosen are 600rpm (quite low force value), 1200rpm (first omega), 1800rpm (second omega), 3800rpm (jump) and 6000rpm (low stabilized force valued).

As far as torque is concerned, for this batch of simulations I set a symmetrical input torque, going from 50Nm to -50Nm and the inversion takes place at 1 second.

Every other parameter, including gear parameters and Simulink configuration properties setup is the same than the previous model and previous batch of simulations.

4.2.2 Simulations results and vibration analysis

The same parameters that were monitored in the previous batch of simulations without torque inversion are also shown in this section.

Starting from the beginning of the signal path we have Subsystem 1 and the instantaneous position between two teeth that is calculated at the end of it. Before entering the lookup table to calculate the STE this value is monitored and checked. In the following lines are reported the results of the simulations ran in order to catch the values of the most important parameters, expressed in the same order than before, starting from the beginning of the system and going down the signal path.

Tests that have been run at a fixed rotational speed (one of the five expressed in the previous section) and the torque has been set to 50Nm and with the inversion, happening at 1s from the start, it has been brought at -50Nm, that will remain the unchanged for all the simulations at different speeds.

4.2.2.1 Speed at 600 rpm As we have seen before the first subsystem the signal encounters is subsystem 1 and it calculates the instantaneous position taking as input just the rotational speed of the gear; the values obtained are reported in Figure 64.

First results depending also on torque are the values of the STE, for this type of simulation the value of STE were collected before and after the torque inversion and put together in a single plot, in order to observe the phenomenon of inversion and its effect to static transmission error. Down here is reported the value of STE simulated with at a speed of 600rpm.

The first thing that comes to the eye is that values of STE are specular for the two cases of sense of rotation, sign that the system is working correctly in both directions. Also it is very clear the effect of inversion in STE variation.

Going on with the analysis of the system we have Subsystem 2 and the calculation of the contributions of force; as it was in the previous model the effect of damped force is way bigger than non damped one, so in the plots I reported here only the contribution of damped force is present. In Figure 66

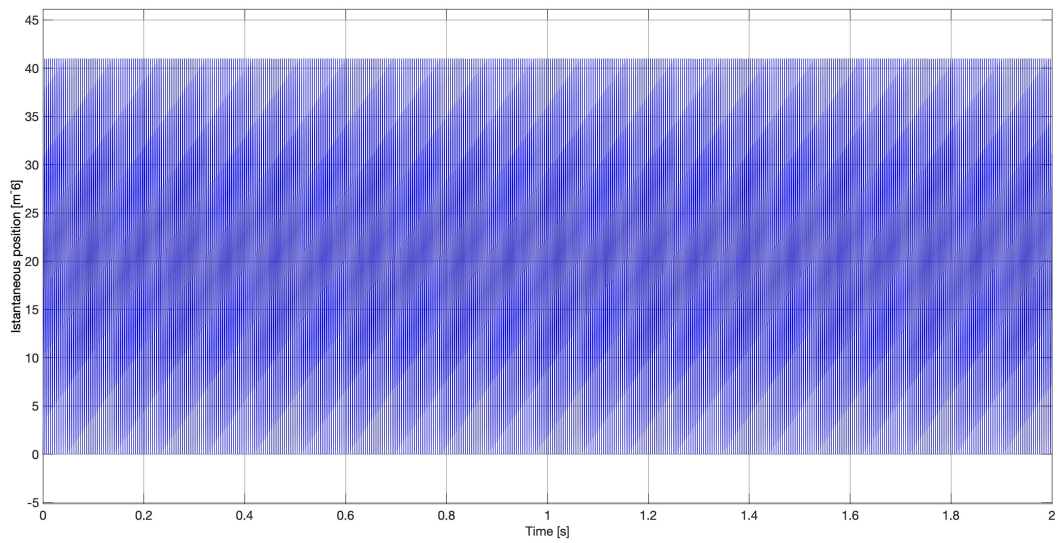


Figure 64: Instantaneous position between two gear teeth coming out of Sub-system 1

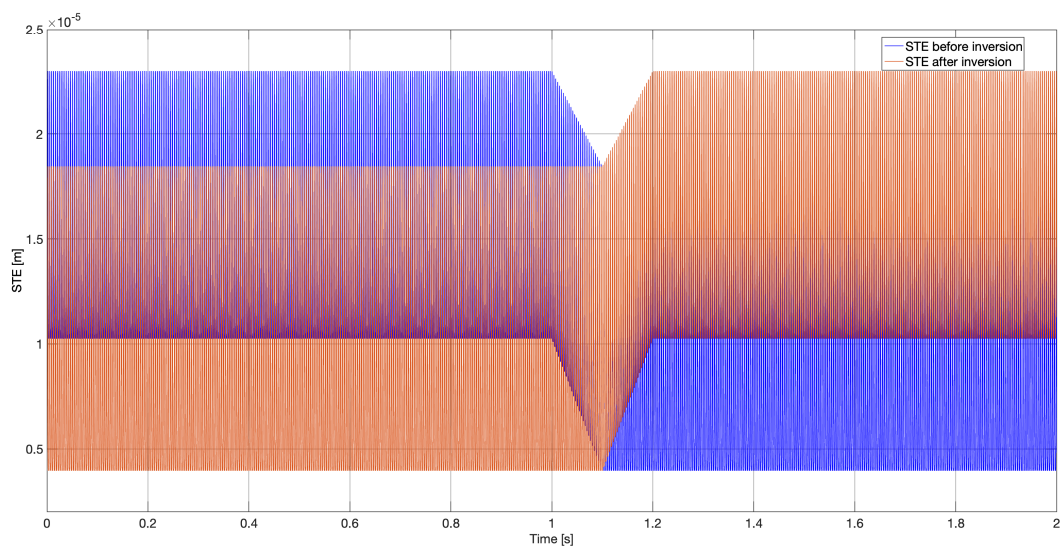


Figure 65: STE values before and after torque inversion at 600rpm

right below we can see the comparison of just the two components of dynamic force that are affected by damping; the main fact that we need to observe is that excluding the time in which we have the inversion of the torque, the two components result exactly equal, this means that the damping effect due to oil film presence works fine in both conditions of rotation, as it was observed for STE.

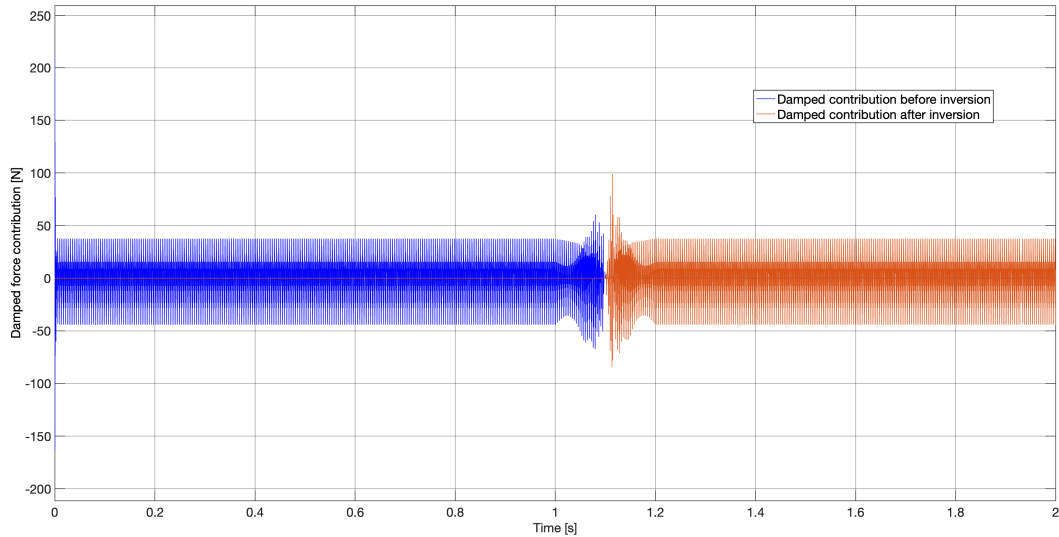


Figure 66: Contribution of damping at 600 rpm, before and after torque inversion

Coming now to the last part of the system we have the final value of the overall dynamic force. As we can see from the plot showed down here in Figure 67 the dynamic force is stable around a certain value until the torque inversion; in the moment in which the torque starts diminishing we can see the force going down to zero and we can observe an oscillation phenomenon taking place.

This phenomenon is fundamental in the study of torque inversion because it represents the two simultaneous contributes of dynamic force in the two motion verses; two inverse dynamic forces are taking place, the one that we have already see before and the second one due to the descending torque and the successive arising of a torque that will make the gear rotate in the opposite direction.

An important observation is that the behavior of the two dynamic force before and after the inversion (so excluding oscillation due to the transition between torques) is perfectly symmetrical, this means that the gears after spinning in the original direction for a while and after undergoing the transition period,

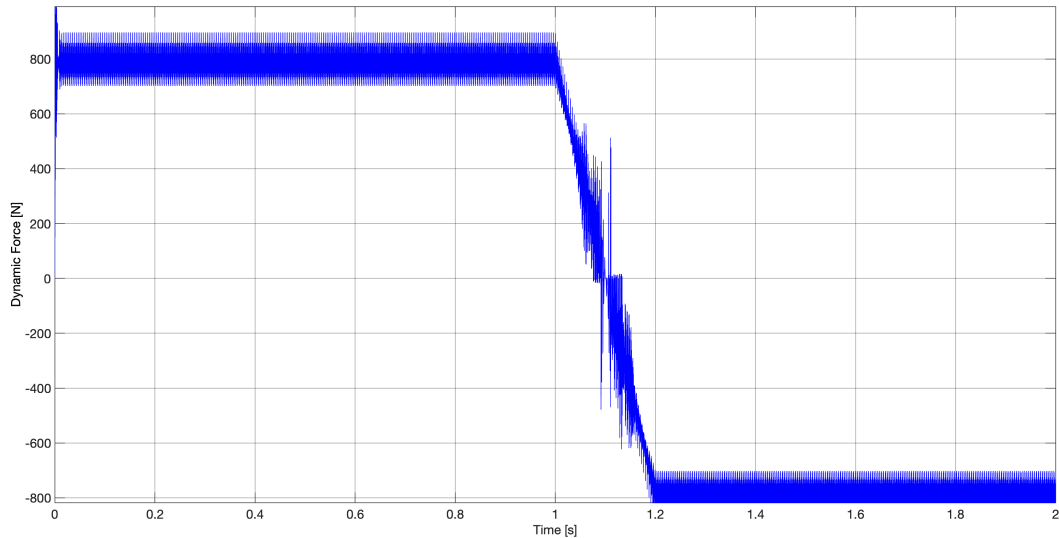


Figure 67: Dynamic force at 600 rpm

start again spinning and exerting the same force in the opposite direction of rotation.

No phenomenon of vibration is seen in the figure, in fact as we can see the values of the force when stabilized are not crossing the zero.

The reason for the lack of vibration is that the dynamic force of this specific system doesn't seem to have resonance phenom at this velocity, so we won't have a peak of force near this rotational speed. Keeping the force value quite low seems to let the system work in a constant contact situation, without contact loss before and after the inversion.

4.2.2.2 Speed at 1200 rpm For this simulation the plot of the instantaneous position of the tooth is shown in Figure 68.

As we can see the range of value isn't different from the one coming out of subsystem 1 in the previous simulations, this happens because the value calculated only depends on the rotational speed and the change of speed will not change the possible positions occupied but only the frequency in which the teeth will occupy a determined position.

Then the values of STE are reported in the plot down below.

The plot is very similar in behaviour to the one at 600rpm, the values are almost equal except for the frequency of oscillation of the STE value, that as we will see in the whole chapter will increase increasing the rotational speed.

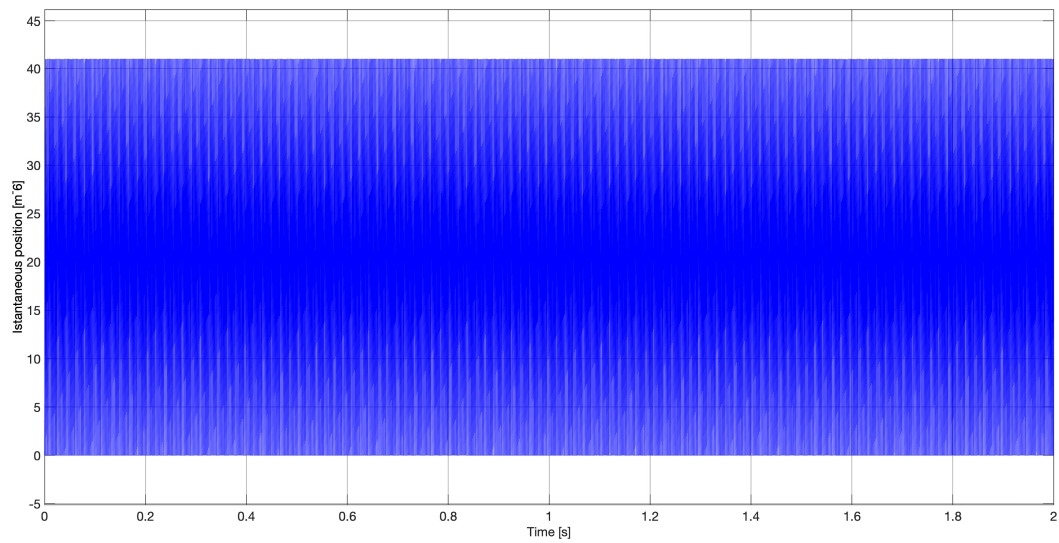


Figure 68: Instantaneous position between two gear teeth coming out of Sub-system 1

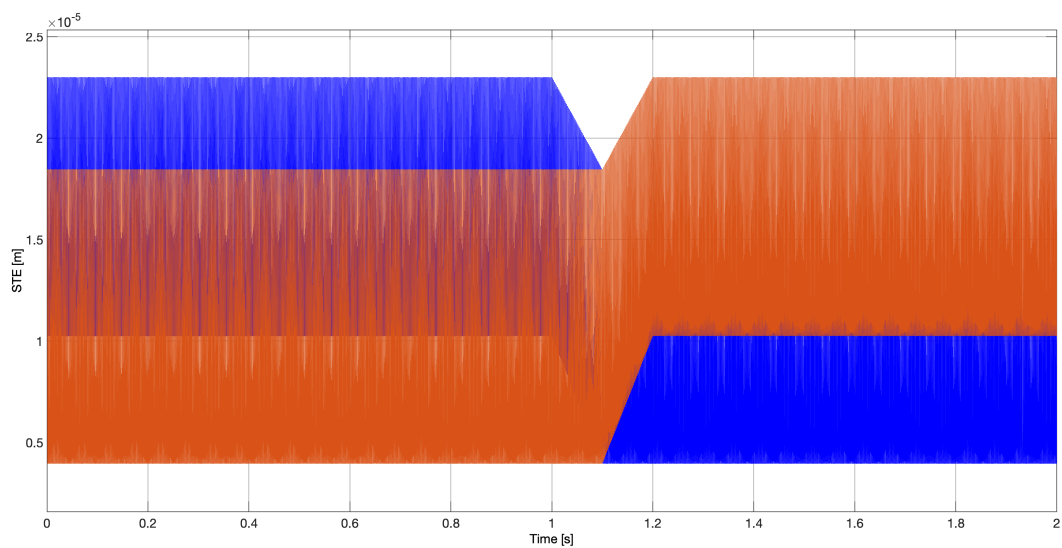


Figure 69: STE values before and after torque inversion at 1200rpm

For what regards different force contributions in Figure 70 is shown the damped contribution of the force, even in this case it is confirmed that damping has the same behaviour before and after the torque inversion.

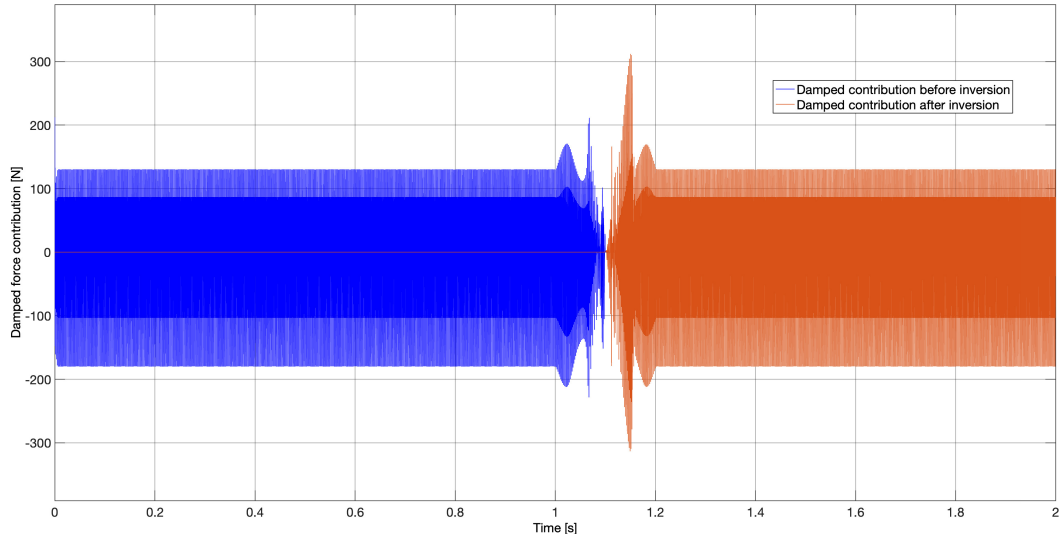


Figure 70: Contribution of damping at 1200 rpm, before and after torque inversion

Finally down here is represented the result of the dynamic force obtained setting a speed of 1200rpm with the same torque and damping factor as before; the plot shows that also in this case the two force are symmetrical and also in this case we can see that vibration is not present neither before or after the inversion.

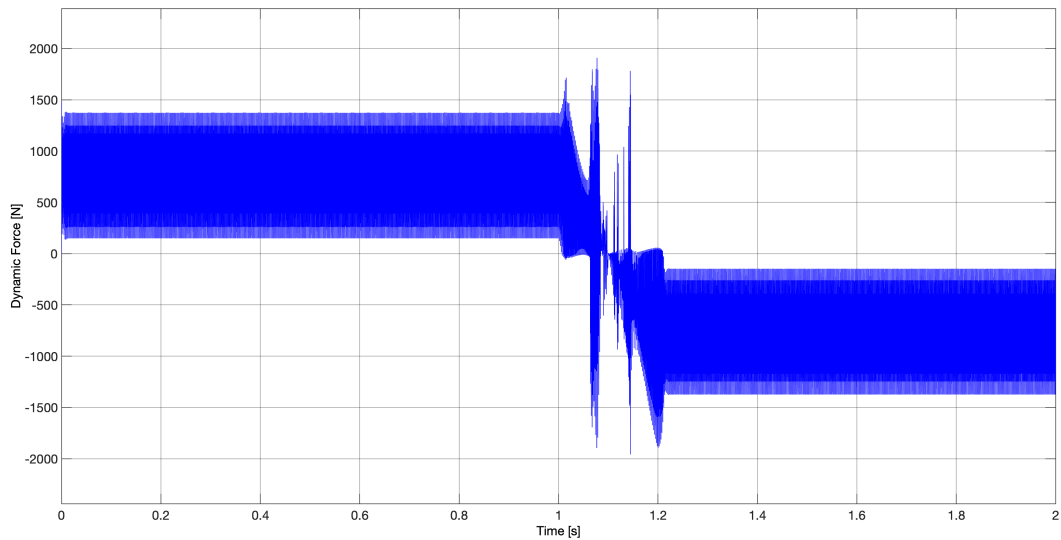


Figure 71: Dynamic force at 1200 rpm

4.2.2.3 Speed at 1800 rpm Increasing the speed we will see the instantaneous position of the teeth changing with higher frequency as depicted in Figure 72.

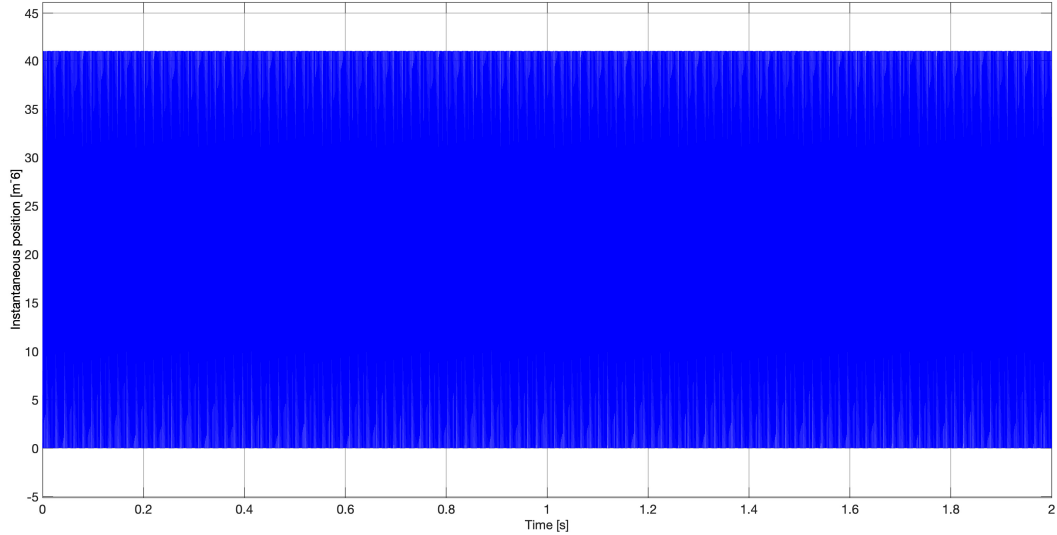


Figure 72: Instantaneous position between two gear teeth coming out of Sub-system 1

Also not much differences in STE plots are showing increasing the speed to 1800rpm, as I said before only the oscillation frequency is increasing as we can see in the following plot.

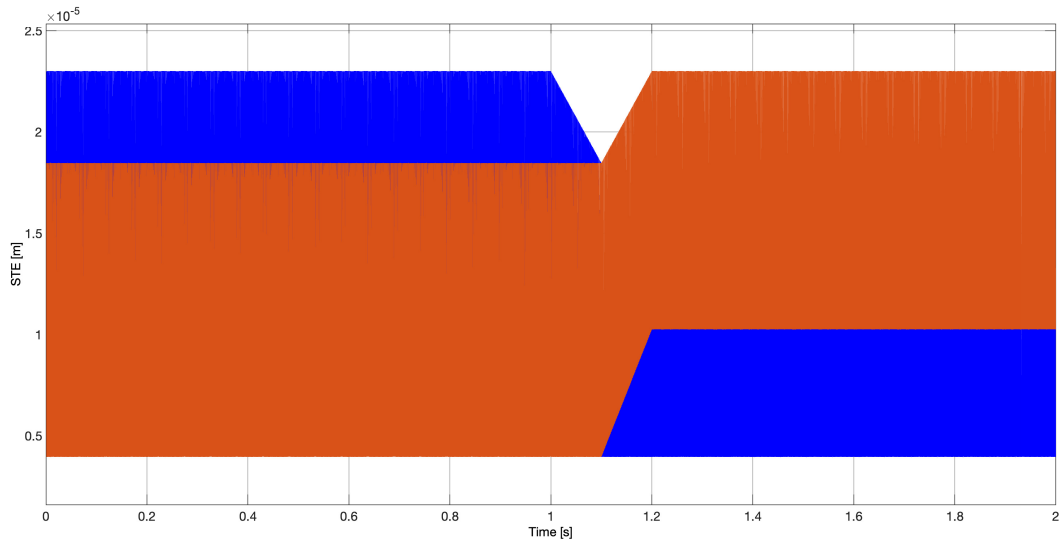


Figure 73: STE values before and after torque inversion at 1800rpm

Also another confirmation is given by the comparison of the two damped force contributions before and after the inversion; Figure 74 shows that also in this case where we have vibration, the two contributions due to damped force are

equal and that factor demonstrate the correct functioning of the Simulink model to calculate every parameter also changing its working conditions.

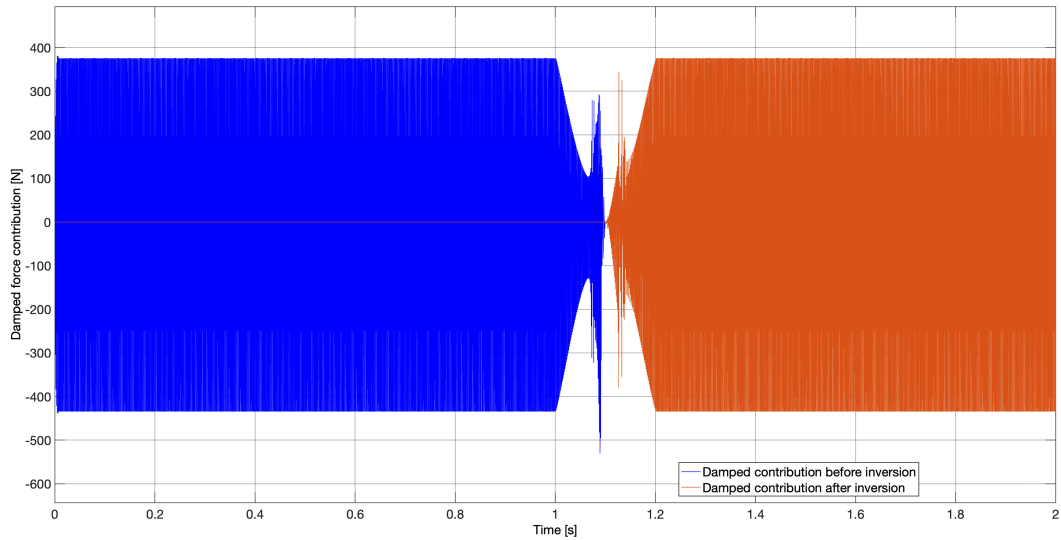


Figure 74: Contribution of damping at 1800 rpm, before and after torque inversion

Very important and completely new for my study instead is the plot shown in Figure 75 because it shows finally vibration of the gears; the plot representing the dynamic force shows in fact that the force itself bounces above and below zero with a certain frequency.

This phenomenon causes contact loss between the two gears that will start vibrate having collisions and contact in both the directions of motion, eventually causing noise and premature wear of the gear.

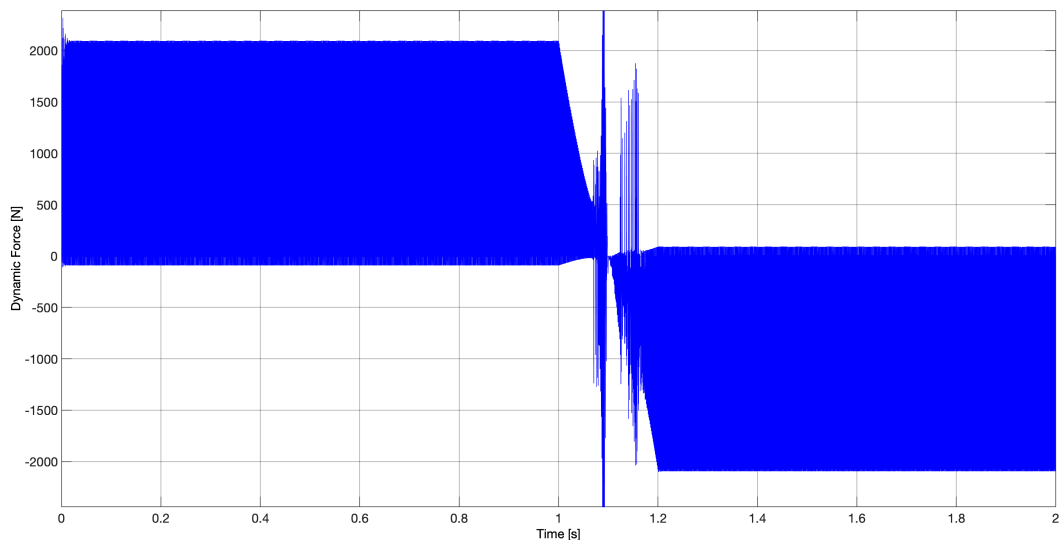


Figure 75: Dynamic force at 1800 rpm

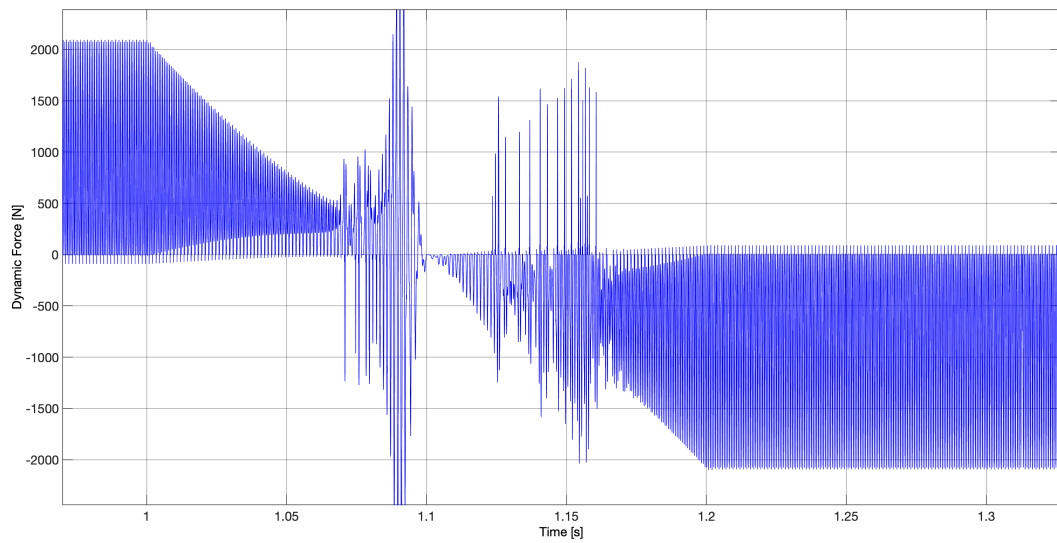


Figure 76: Detail of vibration caused by dynamic force at 1800 rpm

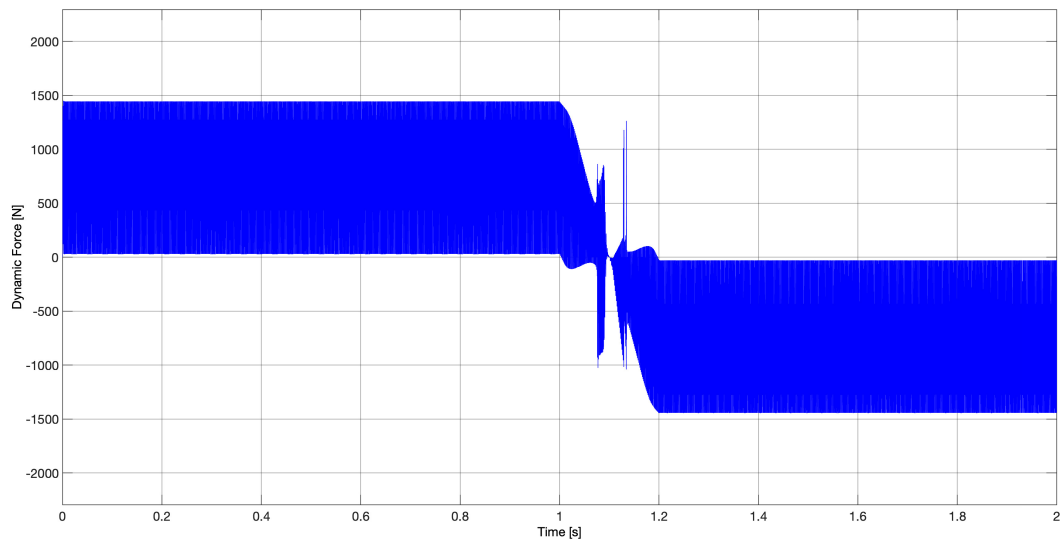


Figure 77: Dynamic force at 1800 rpm without vibration using damping factor 0.14

The presence of this phenomenon is due to the binomial of torque applied and damping factor chosen: in a few words in this specific system with this characteristics using this torque and this damping factor will show vibration, lowering the torque or increasing damping will make this effect disappear as we can see in Figure 77.

In Figure 77 has been found the lowest value of damping factor zeta in order to avoid vibration using a torque of 50Nm at this speed of 1800rpm; the result was $\zeta=0.14$.

For this reason this input data of torque and damping factor were chosen, in order to be able to study this phenom but without having vibration at every rpm, a compromise has been searched.

4.2.2.4 Speed at 3800 rpm Next test has been run with a rotational speed of 3800 rpm, that will again increase the oscillation frequency of instantaneous position and STE values, their behaviours are reported in the next figures.

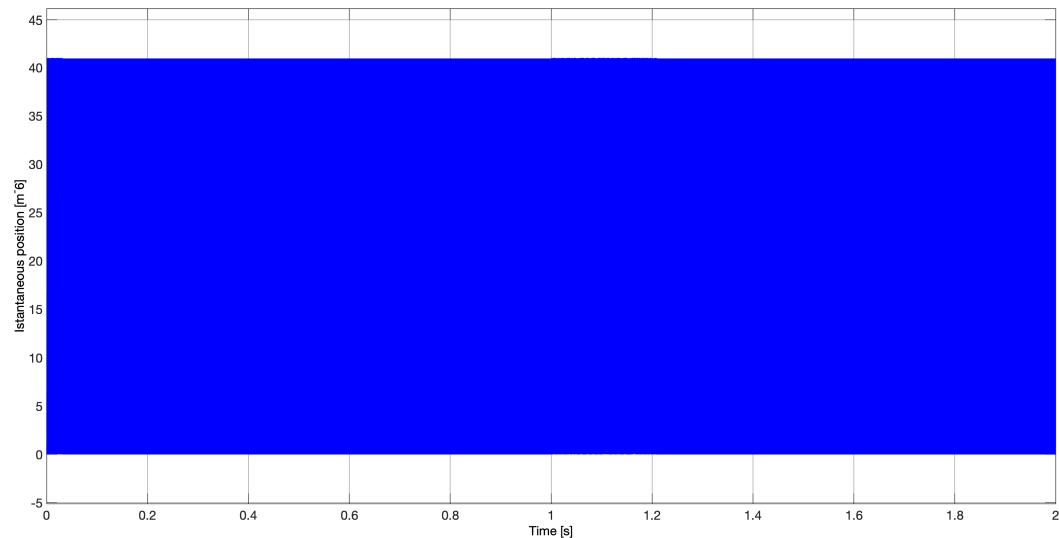


Figure 78: Instantaneous position between two gear teeth coming out of Sub-system 1

Figure 80 reports again the behaviour of the damped component of the dynamic force, no changes in the fact that the two contributions are the same all along the simulation but the time window where the torque inverts.

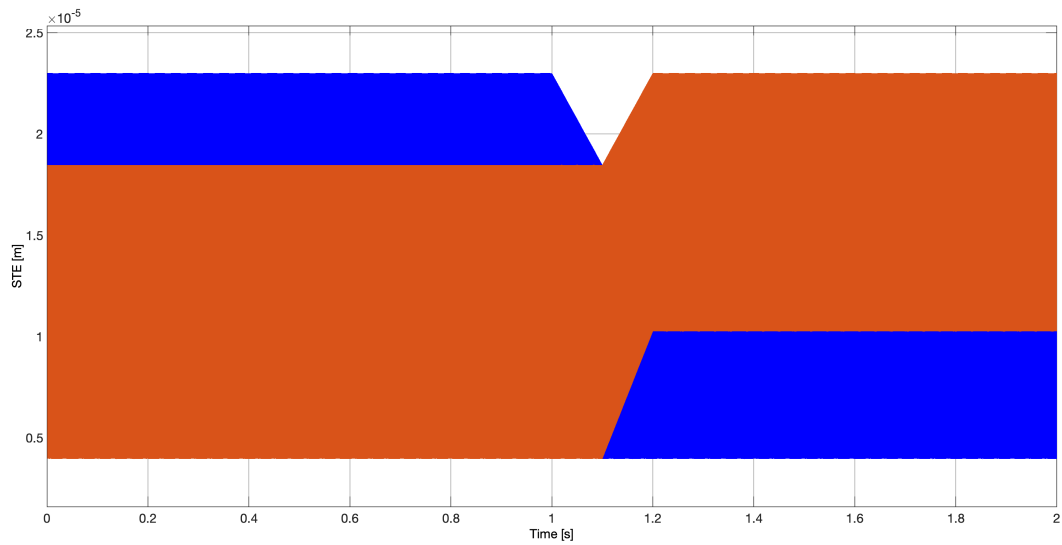


Figure 79: STE values before and after torque inversion at 3800rpm

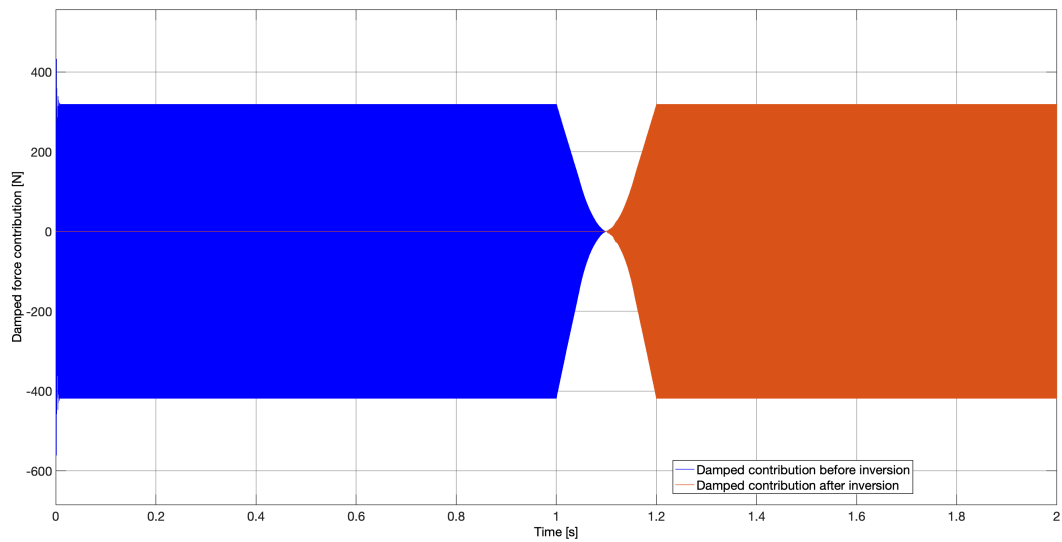


Figure 80: Contribution of damping at 3800 rpm, before and after torque inversion

Coming to the most interesting aspect of all these batch of simulations, here the phenomenon of vibration is even stronger than before. This happens because near this specific speed in the graph representing the dynamic force seen before (Figure 63) we have the jump phenomenon, with the highest peak of force value, that will influence the level of stress peak in the system, making its response to a lower damping factor be just like this.

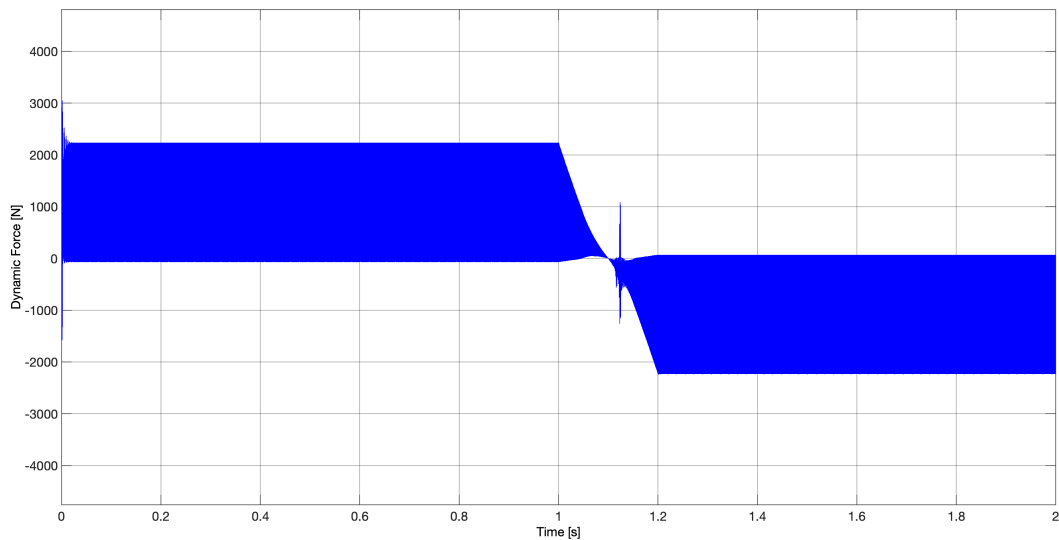


Figure 81: Dynamic force at 3800 rpm

Also a more detailed vision of the value of force oscillating above and below zero causing gear vibration is shown in Figure 82.

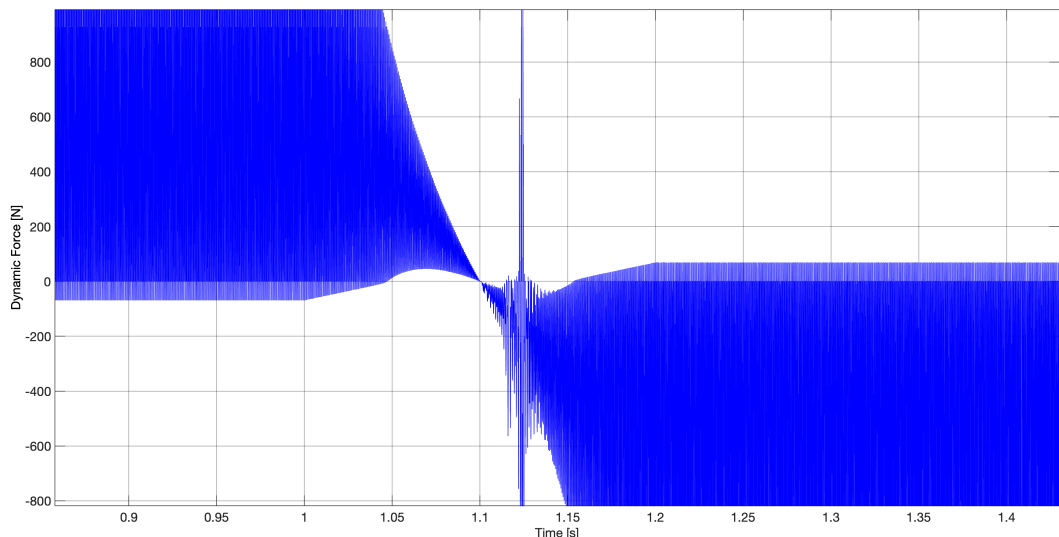


Figure 82: Detail of vibration caused by the dynamic force at 3800 rpm

Because of the jump and the peak of dynamic forces it causes, this quantity of stress is quite difficult to bear without having vibration of gears; as we can see

in Figure (83) I made some tests in order to find the minimum damping factor to apply to this system in order to have a result without vibration keeping unchanged torque and speed, but the resulting damping factor turned out to be $\zeta=0.2$ that is way too high to be applied in a realistic system.

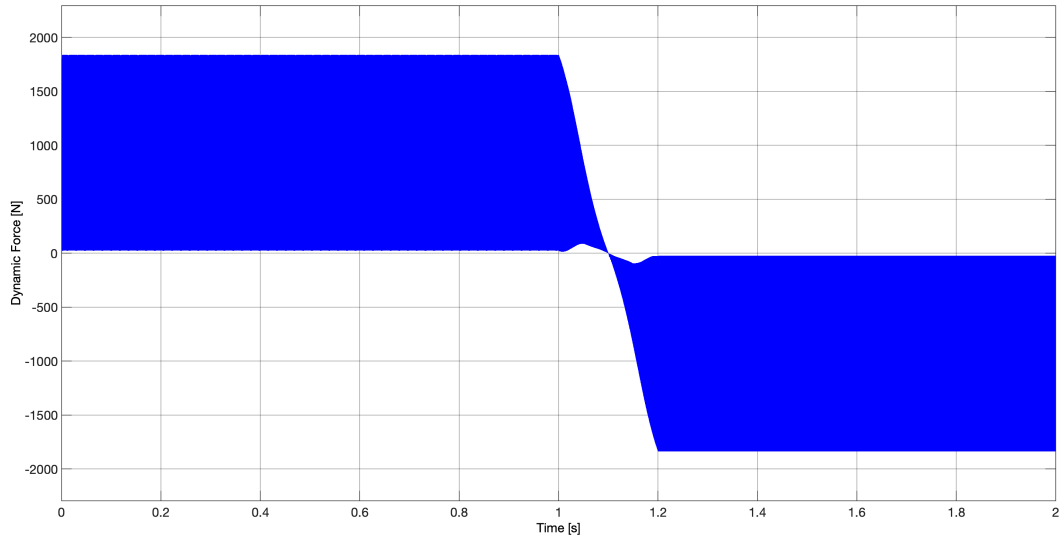


Figure 83: Dynamic force at 3800 rpm without vibration using damping factor=0.2

4.2.2.5 Speed at 6000 rpm Last simulation of the batch has been run at high velocity in order to study what happens when the dynamic force is already stabilized around a certain value and the rotational speed reaches quite high values (at least considering parameters proper of this system) so the rotational speed chosen for the last simulation is 6000rpm.

As far as the instantaneous position of the teeth is concerned, not much changes are visible except from the frequency of motion in the plot down below in Figure 84.

For what regards STE, in this case it reaches its maximum oscillation frequency of the entire batch of simulations and we can see it in Figure 85.

Another good confirm of the correct calculation of forces is given by the plot right below, where we can state as for any other simulation that the contribution of damping works in the same way for both working condition of this model.

Looking at the results of the overall dynamic force (Figure 87) the first thing that comes to the eye is that the phenomenon of vibration is gone; this is due to the fact that at this speed the force is not so high, in fact it stabilized at

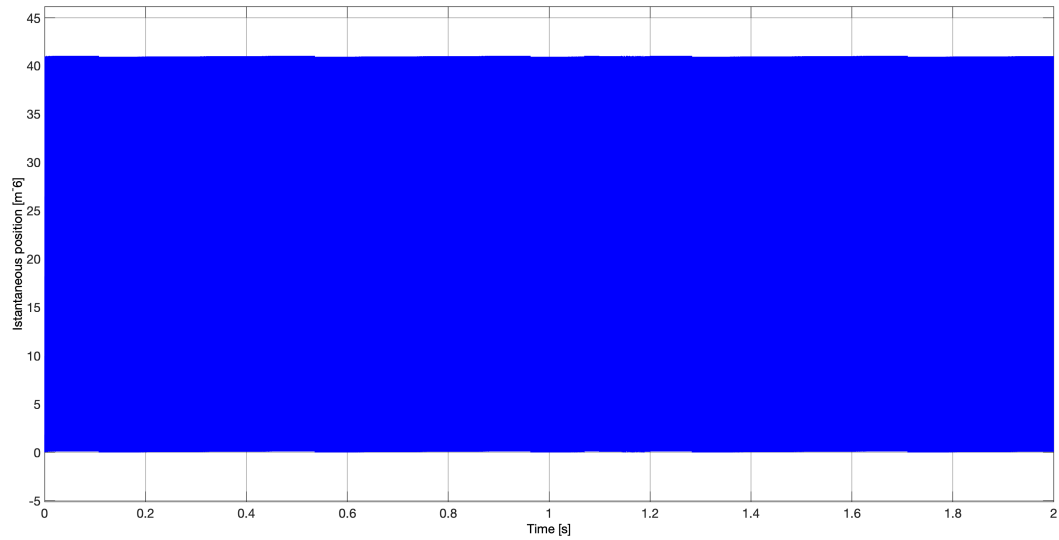


Figure 84: Instantaneous position between two gear teeth coming out of Sub-system 1

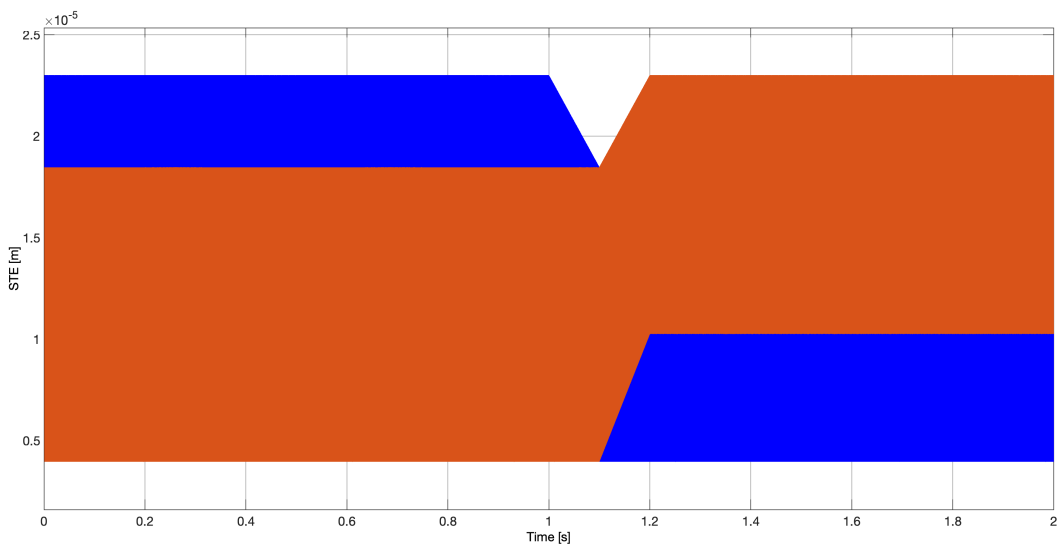


Figure 85: STE values before and after torque inversion at 6000rpm

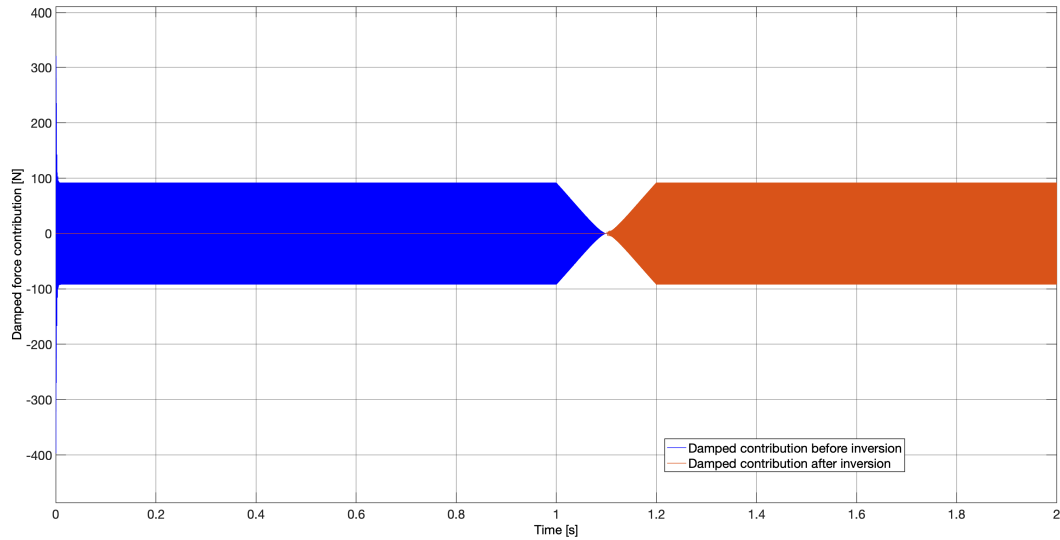


Figure 86: Contribution of damping at 6000 rpm, before and after torque inversion

around 4400 rpm to a quite low value and so it is in the graph of dynamic force considering torque inversion.

This is a further confirm of what stated before, there is a strong relationship between the presence of resonance at certain speeds and the presence of peaks of dynamic force; the changing of the input torque or the damping factor will influence the valued of the force itself but not the moment or the velocity at which a peak will take place.

A quite strong peak of force is present when the torque inversion is almost complete and this can be caused by the fact that in this model the inertia contribute is very low, in fact only the two gears are present without any other element of a more realistic system that would contribute to damp this peaks of force due to inversion.

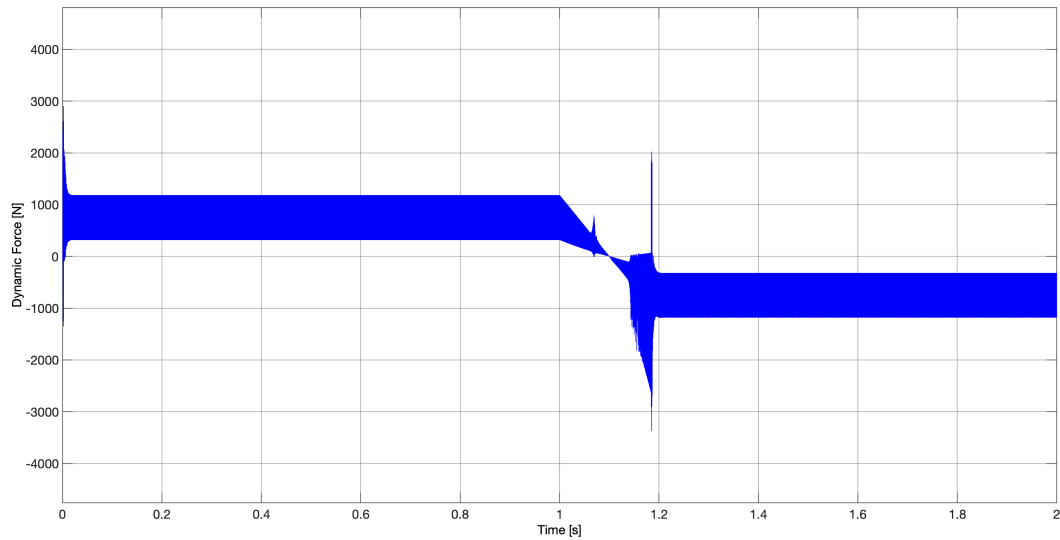


Figure 87: Dynamic force at 6000 rpm

4.3 Further simulations

At the end of this work I also made some further simulations in order to study the behaviour of the system in other different environments and functioning; I wanted to test the model created with different inputs and see if it would remain reliable in calculations.

For this reason I created two more input subsystems; the first one with a step input both for torque and speed, simulating a "real gearbox" in which for each gear there are fixed ranges of torque and rotational speed related to each other. The second one will simulate a more random input, with more than one torque inversion in an environment of non fixed rotational speed.

4.3.1 Step inputs

The first test I made was, as said before, with steps for torque and speed related to each other. The input torques were varied between 25Nm and 200Nm and at which step of torque I associated a rotational speed varying from 1000rpm to 5000rpm; the input schemes of torque and speed which I created for this simulations are reported in the following lines while all the rest of the model has remained exactly the same than before, both in architecture and mathematical parameters.

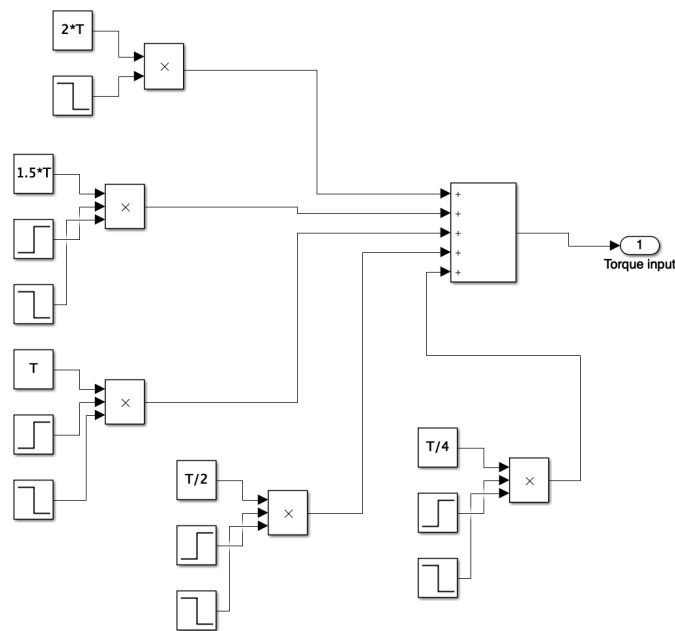


Figure 88: Step input for torque values, T fixed to 100Nm

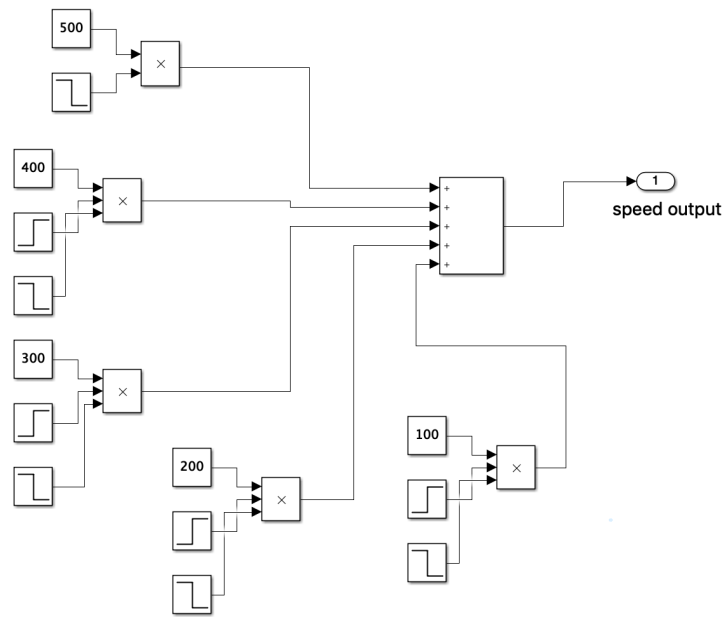


Figure 89: Step input for speed values, every single constant block expresses rotational speed in rad/s

The inputs are characterized by constant values switched on and off by time-actuated steps value, in this way we can have some sort of ladder of values both for torque and speed as shown in Figure 90.

This made me able to have an input in which a value of torque transmitted is associated to a determined speed (something similar to a gearbox functioning); the results of the simulations are reported in the following lines.

Starting from the instantaneous position of the teeth we can see in the graph in Figure 92 that the only parameter changing is the frequency of motion of the position accordingly with the change of speed; this is explained by the fact that the positions that can be occupied only depends on geometrical parameters of the gears, in fact the value range is the exact same of the one in previous simulations.

Going on along the signal path we have the value of STE, differently from before, this value also depends on torque so the pattern of its values along the simulation is represented by a ladder with increasing range of values as long as both torque and speed decrease.

The opposite behaviour is shown instead by the dynamic force, decreasing with the decreasing of torque and speed as depicted in Figure 94.

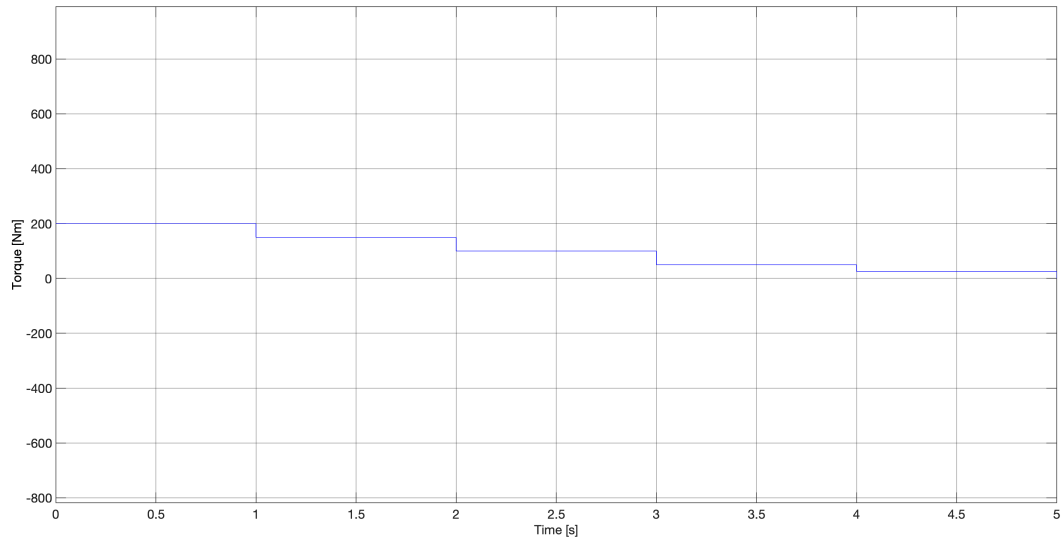


Figure 90: Torque input values

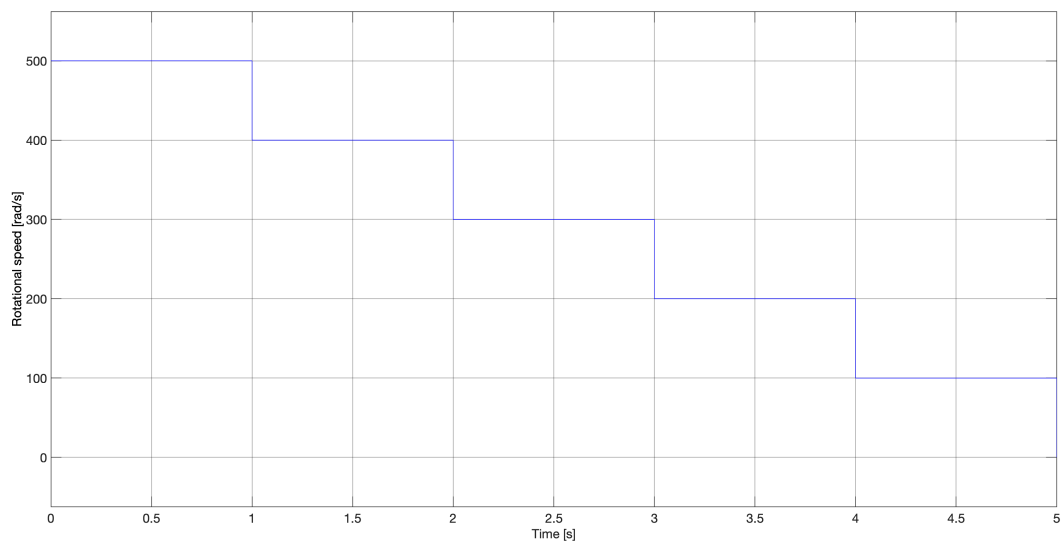


Figure 91: Speed input values

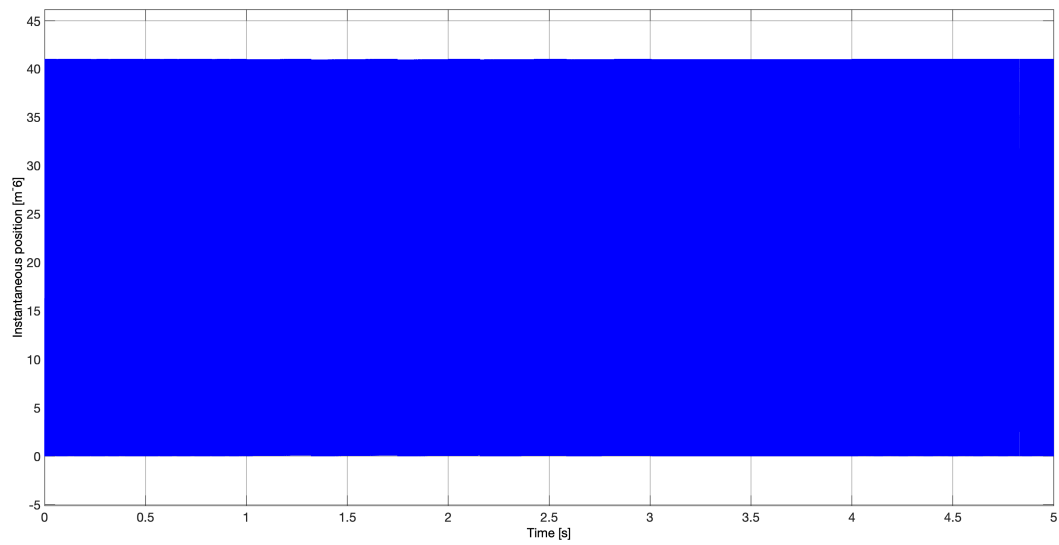


Figure 92: Instantaneous position of the teeth

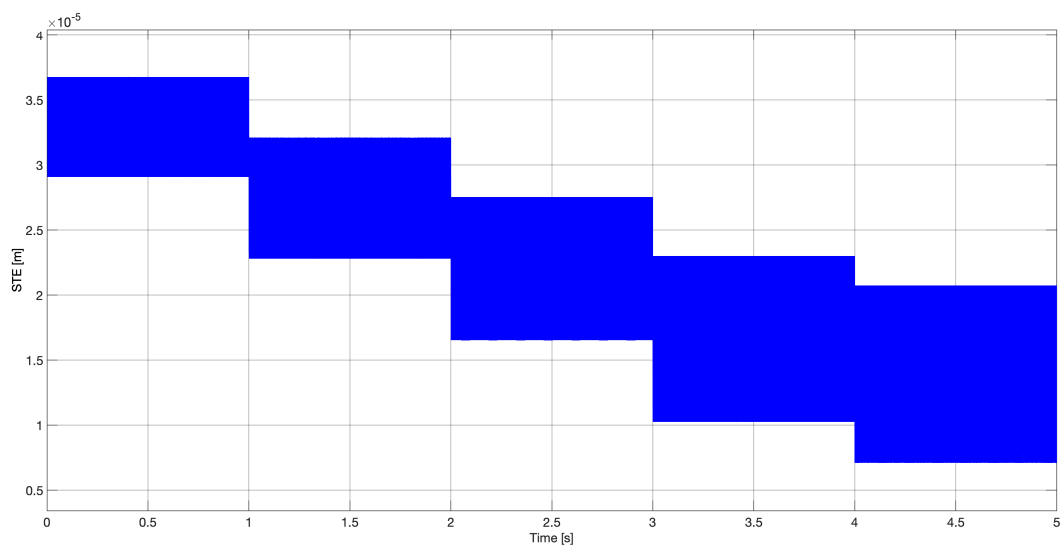


Figure 93: STE values

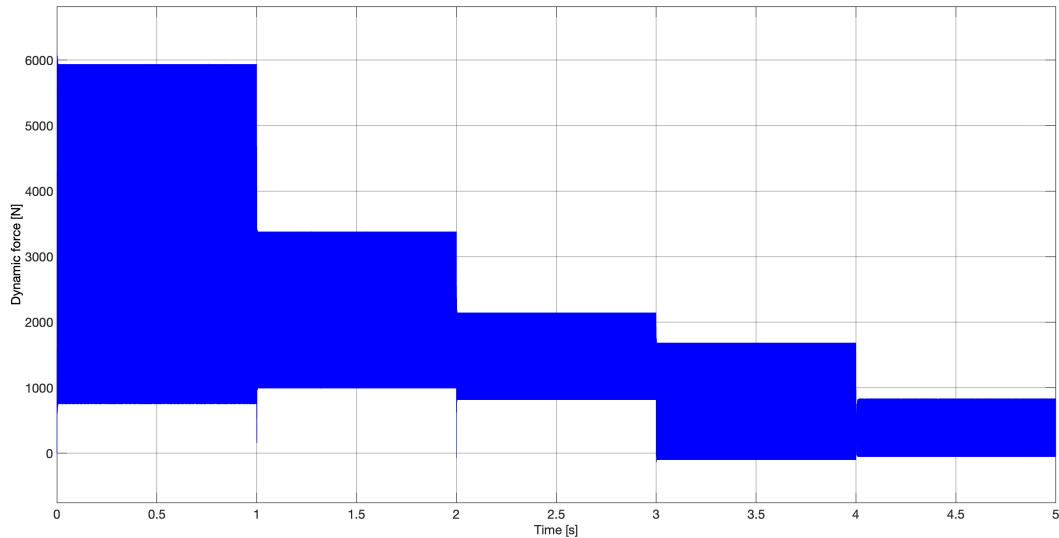


Figure 94: Overall dynamic force

As we can see from the picture the interesting behaviour that the force is showing has a quite large range of oscillation of the force at high torque and speed and step by step it decreases reaching the minimum value at minimum torque and minimum speed. This plot is very important for my work because the shape shown in the picture is quite similar to what happens in a real gearbox, when forces and stresses are very high in low gears and high torques until they reach lower values of torque and speed at higher gears. Also vibration can be seen at very high torque and speed at the beginning of the simulation as well as almost at the end; this is very useful to study the situations of higher stress the gears have to bear and in which conditions they occur.

This is a great result for the explanation of meshing gears' functioning and lots of other tests can be done to this model in order to tweak many more parameters to study the stresses applied to the interested gears and if their functioning remains correct.

4.3.2 Double ramp input

This last test I made is described as "double ramp" because of the input I chose for rotational speed of the system; in fact the input speed is defined by a double ramp that makes the speed increase from zero to a certain level and then decrease again to zero defining the change of the speed in the two directions.

The torque instead is kept constant to 50Nm but inverted to -50Nm and again to 50Nm, all at a quite random timing.

I chose this type of input data in order to test the system in a sort of "random" functioning situation, in order to detect errors in computing the force and other parameters and see how it reacts to an unconventional input (unconventional in a point of view that considers all the previous simulations but overall a more realistic functioning).

Both torque and rotational speed input schemes and their resulting values are reported in figure down below.

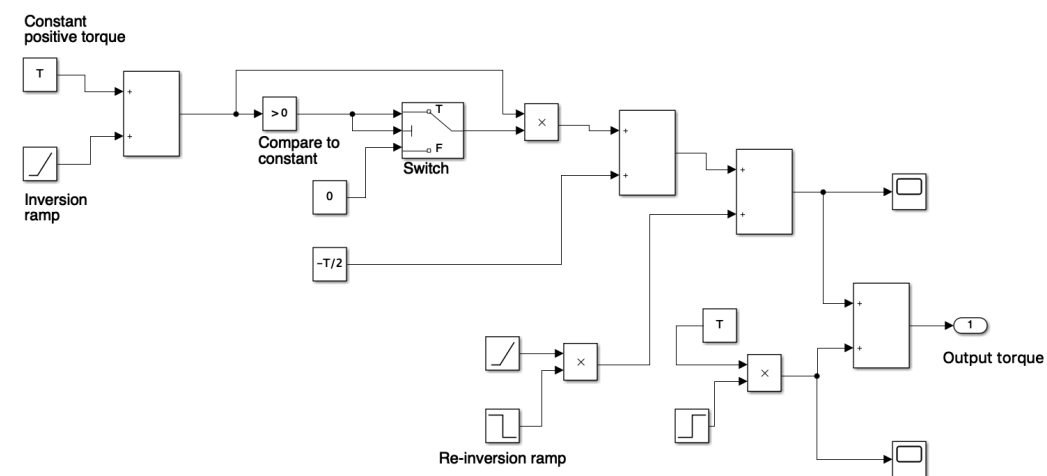


Figure 95: Torque input blocks

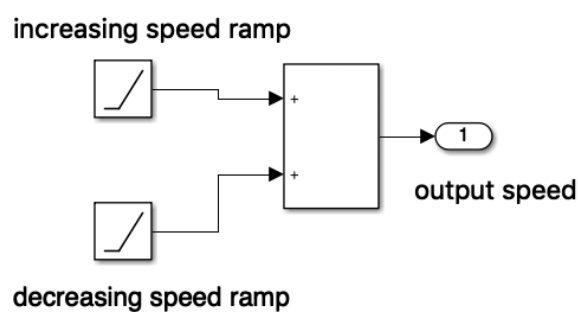


Figure 96: Speed input blocks

Any other parameter of the system hasn't been changed from the previous simulations and simulations have been ran and first result shown is the instantaneous position occupied by the teeth, that as in any other simulation

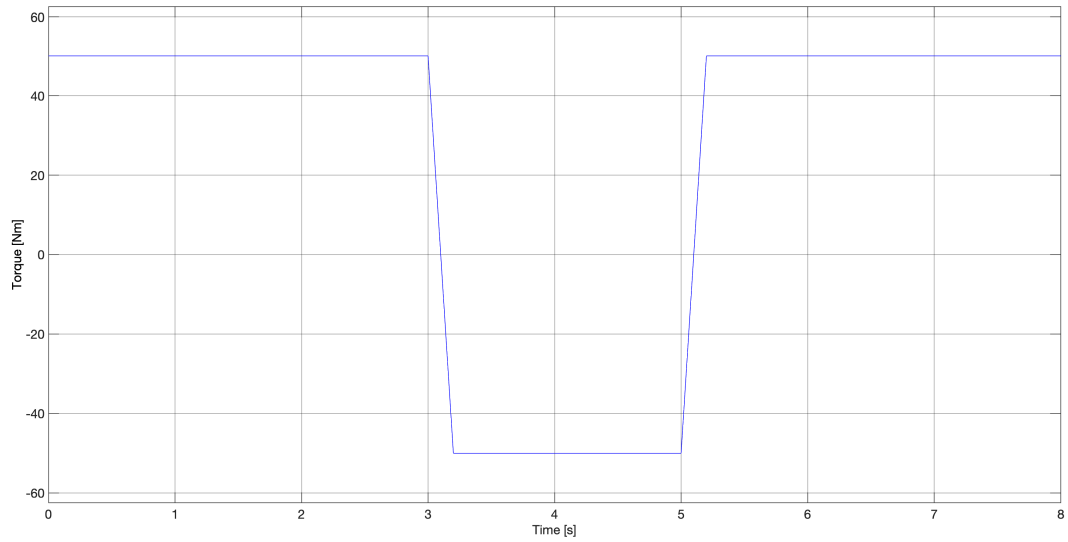


Figure 97: Torque input value

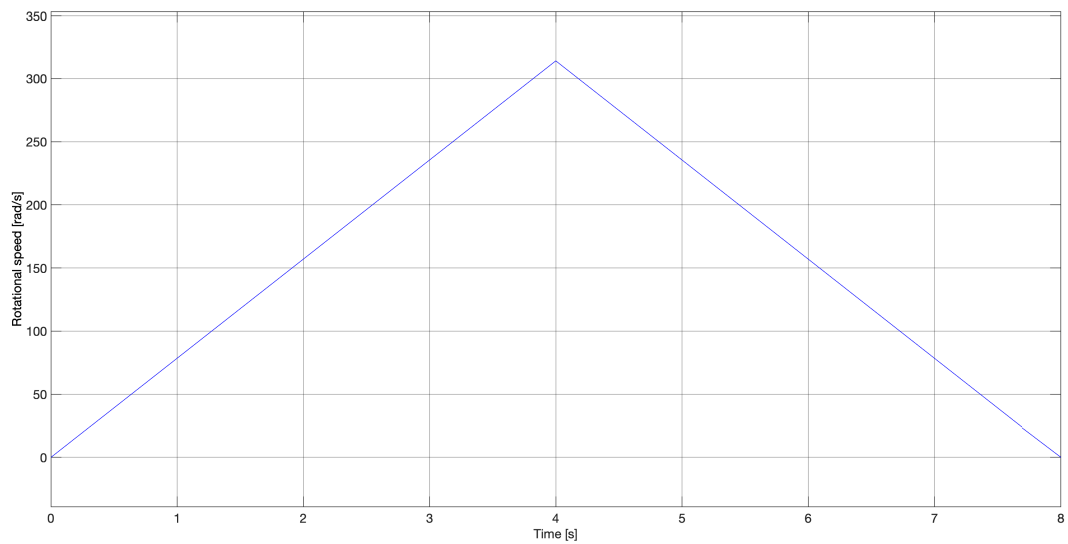


Figure 98: Speed input value

of the batch only depends on speed and geometry of the gear; in fact also in this case the only variation visible is the variation of frequency of oscillation with the variation of speed (Figure 99): higher frequency at the "centre" of the simulation where we have peak of speed and lower frequency where speed has its lower values.

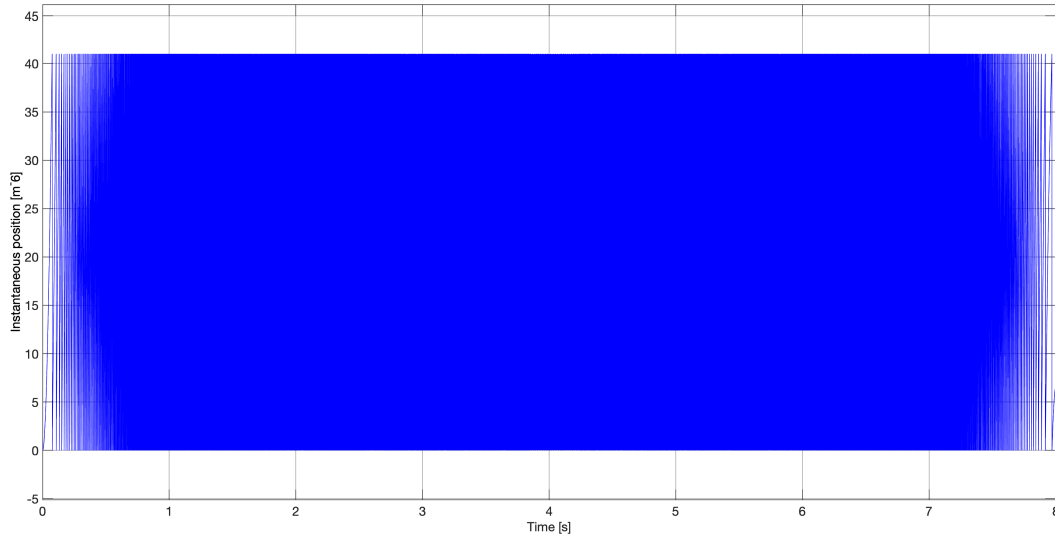


Figure 99: Instantaneous position of the teeth

Then going on along the signal path we have the calculation of STE that is reported down below, showing how the values of STE remains symmetrical before and after the inversion as symbol of good functioning of the model. Also in this case frequency of oscillation is influenced by the value of rotational speed, at the sides of the graph we can see the STE corresponding to lower speeds and going to the center the "high speed" STE frequency.

Last and most important parameter is dynamic force; the plot obtained by the simulation run is depicted in Figure 101 and shows us the functioning of the system with random-ish inputs.

The overall functioning of the model seems confirmed, the moments in which the torque inverts are well visible and clear as the patterns of the dynamic force and the beginning of peaks due to characteristic frequencies are also present; so also with this type of input the model remains reliable and autonomous in detection of data and calculations. An interesting factor is represented by the very high peaks of force in the moment of inversion, due as analyzed before to the lack of inertia terms in the system that will damp this peak a lot (they would presumably vanish adding inertia elements such as wheels or shafts).

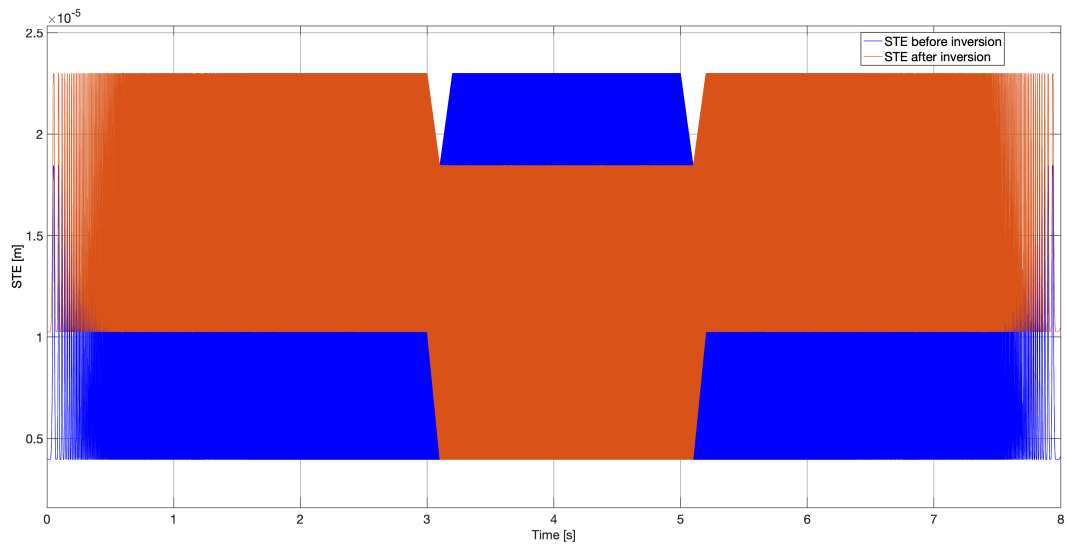


Figure 100: STE before and after torque inversion

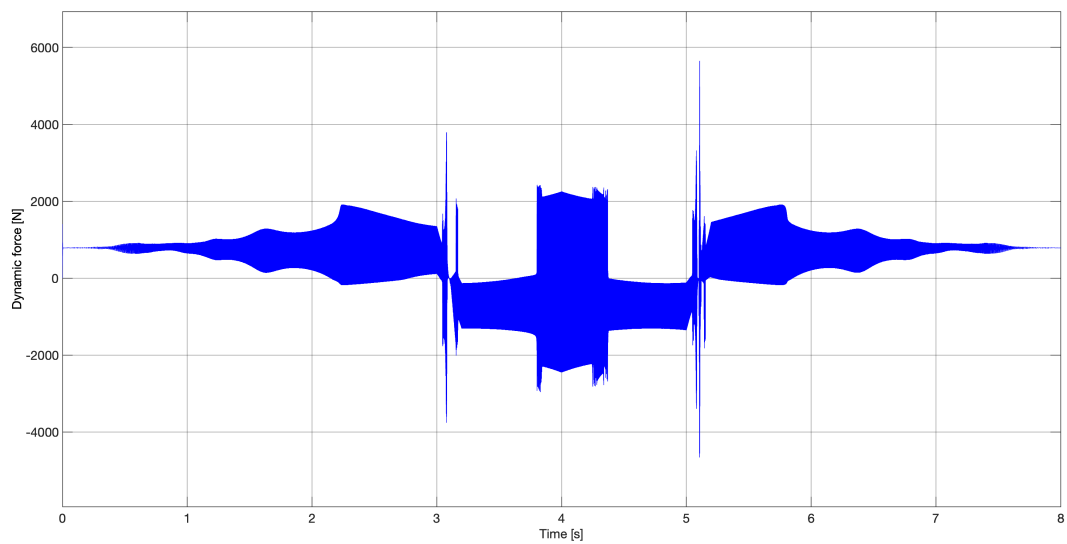


Figure 101: Overall dynamic force

Conclusions

Coming at the end of this work the result is a Simulink model that is able to be fed with whatever torque and speed the user wants, it is able to process the data inserted and calculate many parameters needed for designing geared wheels in total autonomy. The first difficulties regarding the values of torque I was feeding the system with have been overcome and the result is a system that works fine from a theoretical point of view and runs very fast if compared to many other softwares in circulation.

From only two inputs and the geometrical definition of the two meshing gears the model is able to extrapolate static and dynamic parameters, calculate the dynamic force acting between the two gears and monitor many parameters all along the process to come to the dynamic force: gear teeth displacements can be calculated, contributions of damping and stiffness, standard transmission error and many others.

A fundamental aspect that I managed to implement in this model is the ability to detect if the two gears are in a full contact configuration or if lack of contact or even vibration are occurring. This was a fundamental achievement for my work, it represented the most difficult implementation in the system and it opens up a lot of ways to improve the model and to begin new studies on the topic. This function will also be very useful in many future works in order to analyze the full behaviour of meshing gears in even more complex systems.

For this reason I think that the work done to build up this whole system has been a success.

The main difficulties I ran into trying to build this model were due to problem in overcoming Simulink's bonds in mathematical calculations and to make the results coming out of my Simulink model match with results obtained by experimental tests and theoretical aspects of functioning, in order to make my model reliable and to make it as close as possible to the real deal in terms of accuracy and flexibility of usage. Also very tricky was trying to design a layout that would work fine for every input data a random user would want to insert, but that would also run in short time since using a Matlab extension.

Many improvements can be done to this model from the layout point of view, maybe creating custom blocks using mathematical functions that will make the model more accurate and will make architecture of the model lighter and slimmer to understand and also to run. This model can be also included in much

more complex systems, expanding the study on the appearance of gear vibration, the parameters that influence the presence of this phenom and its effects on stress the gears have to bear in order to maintain a correct functioning.

Appendix: Matlab configuration workspace

Here are included all the Matlab settings used to identify the two meshing gears in exam; everything was taken from the original Matlab workspace file that makes the Simulink model run.

Workspace	
Name ▲	Value
alpha	25
arc	0.2244
b	2.5000e-05
c	1.0414e+03
c_gear	100
C_gear	12x12 double
c_input_shaft	1
C_input_shaft	12x12 double
c_pinion	100
C_pinion	12x12 double
c_tooth_gear	100
C_tooth_gear	12x12 double
c_tooth_pinion	100
C_tooth_pinion	12x12 double
cdata	196x530x3 uint8
discretization	196
disp_parker	2813334x2 double
disp_parker1	2813334x2 double
division	10
dotw	78.5400
dt	7.2886e-07
dynforce_parker	2813334x2 double
F	1.5763e+03
Fs	25600
invM_input_shaft	12x12 double
invM_tooth_gear	12x12 double
invM_tooth_pinion	12x12 double
J1	0.0042

Workspace	
Name ▲	Value
tout	20000005x1 dou...
tr	1x70000 double
w	1x27440065 dou...
wn1	1.2339e+04
wn2	1.3623e+04
wn3	1.4425e+04
wn4	1.4994e+04
wn5	1.5449e+04
z1	28
z2	28
zeta	0.0800

Workspace	
Name ▲	Value
J2	0.0042
J_input_shaft	0.2000
J_x	0.0022
J_y	0.0022
J_z	0.0042
k_c	8.0311e+07
k_gear	100000000
K_gear	12x12 double
k_input_shaft	100000000
K_input_shaft	12x12 double
k_pinion	100000000
K_pinion	12x12 double
k_tooth_g	100000000
K_tooth_gear	12x12 double
k_tooth_p	100000000
K_tooth_pinion	12x12 double
km1	400x1 complex d...
km2	400x1 complex d...
km3	400x1 complex d...
km4	400x1 complex d...
km5	400x1 complex d...
m	0.5275
m_e	0.5275
M_gear	12x12 double
m_input_shaft	1
m_pinion	1.4582
M_pinion	12x12 double
m_tooth_g	0.1000

Workspace	
Name ▲	Value
m_tooth_p	0.1000
Model	0
module	0.0050
omega_max	1.5708e+03
out	1x1 SimulationO...
pitch	0.0157
r_b_gear	0.0634
r_b_pinion	0.0634
Rb	0.0634
Rb1	0.0634
Rb2	0.0634
rp1	0.0700
rp2	0.0700
Scope	1x1 Dataset
ScopeREM	20000005x2 dou...
STE	5x40 double
STE1	27439608x2 dou...
STE1R	1x196 double
STE2	27439608x2 dou...
STE2R	1x196 double
STE3	27439608x2 dou...
STE3R	1x196 double
STE4	27439608x2 dou...
STE4R	1x196 double
STE5	27439608x2 dou...
STE5R	1x196 double
T	100
tend	20

References

- [1] (2001). Fundamental rating factors and calculation methods for involute spur and helical gear teeth. *ANSI/AGMA*, (C95).
- [2] Gill-Jeong, C. (2009). Analysis of the nonlinear behavior of gear pairs considering hydrodynamic lubrication and sliding friction. *Journal of Mechanical Science and Technology*, (23):2015–2137.
- [3] Harris, S. L. (1958). Dynamic loads on the teeth of spur gears. *Proceedings of the Institution of Mechanical Engineers*, (172):87–112.
- [4] Kahraman, A. and Blankenship, G. (1995). Steady state forced response of a mechanical oscillator with combined parametric excitation and clearance type non-linearity. *Journal of Mechanical Design, Transactions of the ASME*, (117):743–765.
- [5] Kahraman, A. and Blankenship, G. (1999a). Effect of involute contact ratio on spur gear dynamics. *Journal of Mechanical Design, Transactions of the ASME*, (121):112–118.
- [6] Kahraman, A. and Blankenship, G. (1999b). Effect of involute tip relief on dynamic response of spur gear pairs. *Journal of Mechanical Design, Transactions of the ASME*, (121):313–315.
- [7] Kahraman, A. and Singh, R. (1990). Non-linear dynamics of a spur gear pair. *Journal of Sound and Vibration*, (142):45–79.
- [8] Kahraman, A. and Singh, R. (1991). Interactions between time-varying mesh stiffness and clearance non-linearities in a geared system. *Journal of Sound and Vibration*, (146):135–156.
- [9] Ketter, W., Peters, M., and Collins, J. (2016). A Multiagent Competitive Gaming Platform to Address Societal Challenges. *MIS Quarterly*, 40(2):447–460.
- [10] Li, S. and Kahraman, A. (2007). Effect of sliding friction on the dynamics of spur gear pair with realistic time-varying stiffness. *Journal of Sound and Vibration*, (301):927–949.
- [11] Li, S. and Kahraman, A. (2011a). A spur gear mesh interface damping model based on elastohydrodynamic contact behaviour. *Int. J. Powertrains*, (1).

- [12] Li, S. and Kahraman, A. (June 2011b). Influence of dynamic behaviour on elastohydrodynamic lubrication of spur gears. *Journal of Engineering Tribology*, pages 225–740.
- [13] Ozguven, H. N. and Houser, D. R. (1988a). Dynamic analysis of high speed gears by using loaded static transmission error. *Journal of Sound and Vibration*, (125):71–83.
- [14] Ozguven, H. N. and Houser, D. R. (1988b). Mathematical models used in gear dynamics - a review. *Journal of Sound and Vibration*, (121):383–411.
- [15] R.G. Parker, S. V. and Imajo, T. (2000). Non-linear dynamic response of a spur gear pair: modelling and experimental comparisons. *Journal of Sound and Vibration*, (237):435–455.
- [16] Rosso, P. C. (July 2015). Deliverable D1.1/bis: Verification of Parker and Kahraman Contents 1D models in an Avio application.
- [17] Singh, M. V. . R. (June 2003). Strategies for Modeling Friction in Gear Dynamics. *Journal of Mechanical Design*.
- [18] Tuplin, W. A. (1950). Gear tooth stresses at high speed. *Proceedings of the Institution of Mechanical Engineers*, pages 162–167.
- [19] Vaishya, M. and Singh, R. (2003). Strategies for modeling friction in gear dynamics. *Journal of Mechanical Design*, (125):383–393.
- [20] Wang, C. C. (1978). Rotational vibration with backlash: Part 1. *Journal of Mechanical Design*, (100):363–373.
- [21] Wang, C. C. (1981). Rotational vibration with backlash: Part 2. *Journal of Mechanical Design*, (100):387–397.